MycoKeys 128: 167–195 (2026)
DOI: 10.3897/mycokeys.128.168361

Research Article

Three new species and two new records of *Hydnum* (*Hydnaceae*, *Cantharellales*) from the Dabie Mountains, China

Yonglan Tuo[1,2], Hang Chu[1], Libo Wang[1], Zhengxiang Qi[1], Jiajun Hu[3], Bo Zhang[1,4,5], Yu Li[1,2,5], Xiao Li[1,4,5]

1 *Engineering Research Center of Edible and Medicinal Fungi Ministry of Education, Jilin Agricultural University, Changchun, 130118, China*
2 *Hefei Mycological Valley Innovation Institute, Hefei 231131, China*
3 *College of Life Sciences, Zhejiang Normal University, Jinhua 321000, China*
4 *Sanjiang Fungal Industry Collaborative Innovation Center, Jilin Agricultural University, Changchun 130118, China*
5 *Industrial Development Institute for Plants, Animals and Fungi Integration of Biyang County, Biyang 463799, China*
Corresponding authors: Bo Zhang (zhangbofungi@126.com); Yu Li (fungi966@126.com); Xiao Li (lixiaomugu@126.com)

Abstract

Hydnum (*Hydnaceæ*, *Cantharellales*), one of the edible ectomycorrhizal fungi, is characterized by a spine-bearing hymenophore. It is widely distributed in temperate regions and forms stable symbiotic relationships with *Fagaceæ* and *Pinaceæ*. During a survey of macrofungi in the Dabie Mountains region of China, ten specimens of *Hydnum* were collected. Based on morphological characteristics and phylogenetic analysis using three genetic markers (ITS + nrLSU + *tef*1-α), three new species (*H. luteoalbum*, *H. albodentum*, and *H. albotomentosum*) were identified and described, and two species newly recorded from the Dabie Mountains (*H. berkeleyanum* and *H. pallidomarginatum*) were reported. *H. luteoalbum* is distinguished by a white pileus covered with white tomentum, dagger-shaped or sword-like spines, and broadly ellipsoid basidiospores. *H. albodentum* is characterized by a pale brown pileus and subelliptical basidiospores (8.0–8.5 × 6.0–7.0 µm; av. Q = 1.17). *H. albotomentosum* features smaller basidiocarps, extremely short spines (0.5–2 mm), and globose to subglobose basidiospores. This study enriches the known taxonomic diversity of *Hydnum* and provides a dichotomous key to the species of *Hydnum* in China to facilitate species identification.

Key words: *Hydnum*, morphology, novel taxa, phylogeny, taxonomy

OPEN ACCESS

Academic editor: Bao-Kai Cui
Received: 13 August 2025
Accepted: 17 January 2026
Published: 10 February 2026

Citation: Tuo Y, Chu H, Wang L, Qi Z, Hu J, Zhang B, Li Y, Li X (2026) Three new species and two new records of *Hydnum* (*Hydnaceae*, *Cantharellales*) from the Dabie Mountains, China. MycoKeys 128: 167–195. https://doi.org/10.3897/mycokeys.128.168361

Copyright: © Yonglan Tuo et al.
This is an open access article distributed under terms of the Creative Commons Attribution License (Attribution 4.0 International – CC BY 4.0).

Introduction

The genus *Hydnum* (*Hydnaceæ*, *Cantharellales*), established by Linnaeus in 1753 and typified by *H. repandum* L. (Niskanen et al. 2018), exhibits a transcontinental distribution, occurring in Asia (Cao et al. 2021; Kim et al. 2023; Qin et al. 2024; Su et al. 2024; Zhang et al. 2024), Australia (Massee 1910; McNabb 1971), Europe (Grebenc et al. 2009; Márquez-Sanz et al. 2023), and North America (Banker 1901; Niskanen et al. 2018; Swenie et al. 2018). Morphologically, it is characterized by a monomitic hyphal system, nodose-septate hyphae, 2–6-sterigmate basidia, and subglobose to obovoid-elliptical, smooth, hyaline to subhyaline (basidiospores filled with granular inclusions and oily droplets), thin-walled basidiospores (Hall and Stuntz 1971; Moncalvo

et al. 2006; Niskanen et al. 2018; Swenie et al. 2018). Historically, species delimitation in *Hydnum* has largely depended on morphological traits, including basidiome dimensions, pileus coloration, and basidiospore size and morphology (Banker 1906; Huhtinen and Ruotsalainen 2006; Olariaga et al. 2012). Nevertheless, pronounced morphological characteristic overlaps – especially within the *H. rufescens* complex – have long posed challenges to accurate identification, resulting in an underestimation of the genus's diversity (Sugawara et al. 2022).

The integration of molecular phylogenetics with traditional morphological analyses has substantially advanced our understanding of *Hydnum* diversity. For example, Feng et al. (2016), using multi-marker datasets (ITS, RPB1, and *tef*1-α), revealed at least 31 *Hydnum* species and preliminarily divided them into four groups (*Albomagnum*, *Vesterholtii*, *Rufescens*, and *Repandum*), although systematic taxonomic treatments of these lineages were not provided. Subsequently, Niskanen et al. (2018) combined morphological evidence with ITS data, increasing the number of recognized species worldwide to 49, including 22 newly described taxa. They also proposed a classification framework comprising four subgenera (*Alba*, *Hydnum*, *Pallida*, and *Rufescentia*), four sections (*Hydnum*, *Olympica*, *Magnorufescentia*, and *Rufescentia*), and three subsections (*Mulsicoloria*, *Rufescentia*, and *Tenuiformia*). This infrageneric system was further supported by Cao et al. (2021), who conducted a comprehensive multi-marker phylogenetic analysis (ITS, nrLSU, *tef*1-α, RPB2, and mtSSU), confirmed 17 genera within *Hydnaceæ*, and introduced the new subgenus *Brevispina*. Collectively, these studies highlight the importance of integrative taxonomic approaches in resolving long-standing ambiguities and revealing previously unrecognized diversity within the genus.

Globally, more than 60 *Hydnum* species have been recognized, with 32 described from temperate regions such as Europe and North America (Grebenc et al. 2009; Olariaga et al. 2012; Vizzini et al. 2013; Feng et al. 2016; Márquez-Sanz et al. 2023; Qin et al. 2024). In contrast, records from subtropical regions were historically limited. Prior to 2016, only three species – *H. repandum*, *H. repandum* var. *album*, and *H. rufescens* – were reported from China (Ying and Zang 1994; Zang et al. 1996). In recent years, research on *Hydnum* in China has intensified, with 32 species now reported nationwide, more than half of which were originally described from tropical and temperate regions of the country (Feng et al. 2016; Cao et al. 2021; Qin et al. 2024; Su et al. 2024; Zhang et al. 2024). The Anhui Tianma National Nature Reserve, located in the core area of the Dabie Mountains, represents a critical transitional zone between subtropical and warm-temperate ecosystems in China and is recognized as a key area for biodiversity conservation (Xie et al. 2004; Xu and Pan 2019). However, the distribution of *Hydnum* in this region remains poorly documented, and no comprehensive taxonomic treatment has been published to date.

Based on detailed morphological observations and multi-marker phylogenetic evidence, the present study describes three new species of *Hydnum* and reports two newly recorded *Hydnum* species from the Dabie Mountains. These findings contribute to a more complete understanding of the diversity and distribution of *Hydnum* in subtropical China, particularly within the Dabie Mountains region.

Materials and methods

Specimen collecting

Ten specimens were collected from July to October 2023 in the Tianma National Nature Reserve (31°10'–31°20'N, 115°20'–115°50'E), Anhui Province, China. After we thoroughly documented the fresh macroscopic features, the specimens were oven-dried at 40–45 °C and deposited in the Mycology Herbarium of Jilin Agricultural University (**HJAU**).

Morphological studies

Macroscopic characters were documented using field notes and basidiomata photographs. Colorimetric data followed the Methuen Handbook (Kornerup and Wanscher 1978). For micromorphological analysis, dried specimens were examined under a Carl Zeiss Axio Lab A1 compound microscope (Carl Zeiss AG, Jena, Germany). The micrographs of basidia and basidiospores were acquired using a Zeiss Scope A1 microscope (Carl Zeiss AG, Jena, Germany) (Appendix 2). Specimens (collected from each basidiocarp: five spines, approximately 0.2 cm^2 of pileipellis, and 0.2 cm^2 of stipitipellis) were mounted in a staining solution prepared with 3% (w/v) KOH (Sangan Biotech, Shanghai, China, A610441-0500), supplemented with 1% (w/v) Congo Red (Sangan Biotech, A427695-0500) when necessary. Amyloid reactions were tested using Melzer's reagent [3 g KI (Sangan Biotech, A610443-0050), 1 g I_2 (Sangan Biotech, A500538-0100), 40 g $CCl_3CH(OH)_2$ (Sangan Biotech, A500288-0250), dissolved in 40 mL distilled water]. Spore dimensions (n = 100 per species) were recorded as (a) b–c (d) (with 99% of values falling within the b–c range), where mean length (avg. L) and width (avg. W) were calculated by excluding extreme values; Q denotes the L/W ratio (L: spore length, W: spore width).

DNA extraction, PCR, and sequencing

We extracted genomic DNA from samples using the NuClear Plant Genomic DNA Kit (CoWin Biotech Co., Ltd., Jiangsu, China), following the manufacturer's protocols. We selected the primer pairs ITS1F/ITS4 (White et al. 1990; Gardes and Bruns 1993) and *tef*1F/*tef*1R (Feng et al. 2016) to amplify and sequence the ITS and *tef*1-α markers, respectively. For PCR amplification, we prepared a 25 μL reaction mixture containing 2 μL genomic DNA template, 12.5 μL SanTaq PCR Master Mix (Sangon Biotech, Shanghai, China), 8.5 μL ddH_2O, and 1 μL of each forward and reverse primer (10 μM). The PCR cycling parameters were set as follows: initial denaturation at 95 °C for 4 min, followed by 35 cycles of 45 s at 95 °C, 45 s at 56 °C, and 1.5 min at 72 °C, with a final extension at 72 °C for 10 min for ITS; and 95 °C for 3 min, followed by 35 cycles of 40 s at 95 °C, 45 s at 56 °C, and 1.5 min at 72 °C, with a final extension at 72 °C for 7 min for *tef*1-α. After amplification, PCR products were purified with the Genview High-Efficiency Agarose Gels DNA Purification Kit (Gen-View Scientific Inc., Galveston, TX, USA). Purified amplicons were then subjected to Sanger sequencing by Comate Bioscience Co., Ltd. (Jilin, China). Sequence assembly was performed using SeqMan software (DNASTAR, v7.1), and the consensus sequences were deposited in the NCBI GenBank database.

Phylogenetic analyses

The newly generated sequences have been deposited in the National Center for Biotechnology Information (NCBI) database (https://www.ncbi.nlm.nih.gov/). The sequences for the multi-marker (ITS–nrLSU–*tef*1-α) phylogenetic tree were derived from previous studies (Feng et al. 2016; Cao et al. 2021; Qin et al. 2024; Su et al. 2024; Zhang et al. 2024) and highly relevant taxonomic unit sequences identified via BLAST searches (coverage: 97–100% and identity: 97–100%) (Table 1). *Sistotrema muscicola* (Nilsson et al. 2006) was used as the outgroup. The workflow included (1) independent alignments of the ITS, nrLSU, and *tef*1-α sequences, which were aligned in batches with MAFFT v7.505 (Katoh and Standley 2013) using the auto strategy and normal alignment mode; and (2) the sequence alignments were manually adjusted in BioEdit v7.1.3 (Hall 1999). Subsequently, the ITS, nrLSU, and *tef*1-α regions were concatenated using the sequence concatenation tool in the Alignment toolbar of PhyloSuite v1.2.3 (Xiang et al. 2023); (3) ModelFinder v2.2.0 (Kalyaanamoorthy et al. 2017) was used to select the best-fit model using the BIC criterion; (4) Bayesian inference was performed using MrBayes v3.2.7a (Ronquist et al. 2012) with 5 million generations (sampling every 2000 generations, 25% burn-in, and split frequency = 0.004); (5) maximum likelihood analysis was performed using IQ-TREE v2.2.0 (Nguyen et al. 2015) with 4950 ultrafast bootstraps, as well as the Shimodaira–Hasegawa-like approximate likelihood-ratio test (Guindon et al. 2010); and (6) the tree was visualized for topological structure using the online platform ITOL v7.2.1 (https://itol.embl.de). The phylogenetic tree, macroscopic photographs, and microscopic photographs were edited and typeset using Adobe Illustrator 2020 (Adobe, San Jose, CA, USA). In accordance with phylogenetic reporting standards (Leebens-Mack et al. 2006), we deposited the results of phylogenetic analyses (BI and ML trees) and alignment data of concatenated sequences into the online database figshare (https://doi.org/10.6084/m9.figshare.29858450, V2).

Table 1. Specimens and sequences used in this study.

Species	Specimen voucher	GenBank No.			Country	References
		nrLSU	ITS	*tef*1-α		
H. albertense	H T. Niskanen 11-354 (**T**)	–	KX388664	–	Canada	(Niskanen et al. 2018)
H. albodentum	**FJAU66580 (T)**	**–**	**PV997562**	**PX026328**	**China**	**This study**
H. albodentum	**FJAU66581**	**–**	**PV997563**	**PX026329**	**China**	**This study**
H. albomagnum	AFTOL-ID 471	AY700199	DQ218305	DQ234568	USA	(Swenie et al. 2018)
H. albomagnum	RAS231 (**T**)	–	MH379943	–	USA	(Swenie et al. 2018)
H. albomarginatum	FJAU66574 (**T**)	PV356813	PV329855	PP357262	China	(Tuo et al. 2025)
H. albomarginatum	FJAU66575	PV356814	PV329856	PP357263	China	(Tuo et al. 2025)
H. albotomentosum	**FJAU66568 (T)**	**–**	**PV329851**	**PP357256**	**China**	**This study**
H. albotomentosum	**FJAU66569**	**–**	**PV329852**	**PP357257**	**China**	**This study**
H. atlanticum	AJ1597 (**T**)	–	OQ235218	OQ236553	Canada	(Justo et al. 2023)
H. atlanticum	AJ1558	–	OQ235214	OQ236551	Canada	(Justo et al. 2023)
H. berkeleyanum	CAL1656 (**T**)	NG070500	NR158533	–	India	(Wang et al. 2018)
H. berkeleyanum	**FJAU66576**	**–**	**PV875855**	**PV889364**	**China**	**This study**
H. berkeleyanum	**FJAU66577**	**–**	**PV875856**	**PV889365**	**China**	**This study**
H. bifurcatum	FJAU66562 (**T**)	–	PV329845	PP357252	China	(Tuo et al. 2025)

Species	Specimen voucher	GenBank No.			Country	References
		nrLSU	ITS	*tef*1-α		
H. bifurcatum	FJAU66563	–	PV329846	PP357253	China	(Tuo et al. 2025)
H. boreorepandum	HTN1679	–	KX388658	–	Finland	(Niskanen et al. 2018)
H. boreorepandum	H6003711 (**T**)	–	KX388657	–	Finland	(Niskanen et al. 2018)
H. brevispinum	IFP 019464 (**T**)	MW979559	MW980578	–	China	(Cao et al. 2021)
H. brevispinum	IFP 019465	MW979560	MW980579	–	China	(Cao et al. 2021)
H. canadense	HTN09006 (**T**)	–	KX388681	–	Canada	(Niskanen et al. 2018)
H. crassipedum	FJAU66572 (**T**)	PV356811	PV329853	PP357260	China	(Tuo et al. 2025)
H. crassipedum	FJAU66573	PV356812	PV329854	PP357261	China	(Tuo et al. 2025)
H. cremeoalbum	TUMH40462	–	AB906674	–	Japan	(Niskanen et al. 2018)
H. cremeoalbum	TUMH60740 (**T**)	–	AB906678	–	Japan	(Niskanen et al. 2018)
H. cuspidatum	RAS246 (**T**)	–	MH379944	–	USA	(Swenie et al. 2018)
H. cuspidatum	RAS205	–	MH379936	–	USA	(Swenie et al. 2018)
H. ellipsosporum	FD3281	KX086217	KX086215	–	Switzerland	(Ostrow and Beenken 2004)
H. ellipsosporum	HTN 12036	–	KX388671	–	Finland	(Niskanen et al. 2018)
H. ferruginescens	MH16005 (**T**)	–	MH379905	–	USA	(Swenie et al. 2018)
H. ferruginescens	RAS229	–	MH379942	–	USA	(Swenie et al. 2018)
H. flabellatum	Yuan14708 (**T**)	MW979556	MW980575	–	China	(Cao et al. 2021)
H. fulvostriatum	FJAU66566 (**T**)	PV356807	PV329849	–	China	(Tuo et al. 2025)
H. fulvostriatum	FJAU66567	PV356808	PV329850	–	China	(Tuo et al. 2025)
H. ibericum	BIO:Fungi:12330 (**T**)	–	HE611086	–	Spain	(Olariaga et al. 2012)
H. ibericum	MA-fungi 3457	–	AJ547879	–	Spain	(Grebenc et al. 2009)
H. jussii	Yuan14008	MW979539	MW980553	MW999436	China	(Cao et al. 2021)
H. jussii	Yuan14009	MW979540	MW980554	MW999437	China	(Cao et al. 2021)
H. luteoalbum	**FJAU66564 (T)**	**–**	**PV329847**	**PP357254**	**China**	**This study**
H. luteoalbum	**FJAU66565**	**–**	**PV329848**	**PP357255**	**China**	**This study**
H. magnorufescens	voucher 161209	KU612669	KU612549	–	Slovenia	(Feng et al. 2016)
H. magnorufescens	TOHG2818 (**T**)	–	KC293545	–	Italy	(Vizzini et al. 2013)
H. melitosarx	HTN11056 (**T**)	–	KX388683	–	USA	(Niskanen et al. 2018)
H. melitosarx	K 176869	–	KX388685	–	UK	(Niskanen et al. 2018)
H. melleopallidum	SMI356 (**T**)	–	FJ845406	–	Canada	(Vizzini et al. 2013)
H. mulsicolor	LJUGIS1336 (**T**)	–	AJ547885	–	Slovenia	(Grebenc et al. 2009)
H. mulsicolor	REB341	–	JX093560	–	USA	(Baird et al. 2013)
H. neorepandum	HTN100-95 (**T**)	–	KX388659	–	Canada	(Niskanen et al. 2018)
H. neorepandum	HTN100-86	–	KX388660	–	Canada	(Niskanen et al. 2018)
H. olympicum	H T. Niskanen 09-134 (**T**)	–	KX388661	–	USA	(Niskanen et al. 2018)
H. olympicum	SAT-10-208-05	–	MT955159	–	USA	(Cao et al. 2021)
H. oregonense	HVM61	–	KF879509	–	USA	(Moeller et al. 2014)
H. oregonense	PNMSg2010502h109 (**T**)	–	AJ534972	–	USA	(Grebenc et al. 2009)
H. orientalbidum	TUMH:64068	–	LC621862	–	Japan	(Sugawara et al. 2022)
H. orientalbidum	FJAU66570	PV356809	PV329857	PP357258	China	(Tuo et al. 2025)
H. orientalbidum	FJAU66571	PV356810	PV329858	PP357259	China	(Tuo et al. 2025)
H. ovoideisporum	voucher71106	–	KU612536	–	Slovenia	(Cao et al. 2021)
H. ovoideisporum	BIO Fungi12683 (**T**)	–	NR119818	–	Spain	(Olariaga et al. 2012)
H. pallidocroceum	Yuan14017 (**T**)	MW979554	MW980568	MW999449	China	(Cao et al. 2021)
H. pallidocroceum	Yuan14023	MW979555	MW980569	MW999450	China	(Cao et al. 2021)
H. pallidomarginatum	Yuan13928a (**T**)	MW979552	MW980566	MW999447	China	(Cao et al. 2021)
H. pallidomarginatum	**FJAU66578**	**–**	**PV875857**	**PV889366**	**China**	**This study**
H. pallidomarginatum	**FJAU66579**	**–**	**PV875858**	**PV889367**	**China**	**This study**
H. pinicola	SFC20180928-18	OR211401	OR211383	OR220059	Korea	(Kim et al. 2023)

Species	Specimen voucher	GenBank No.			Country	References
		nrLSU	ITS	*tef*1-α		
H. quebecense	HTN 10-064 (**T**)	–	KX388662	–	Canada	(Niskanen et al. 2018)
H. quebecense	CN9	–	MH379881	–	USA	(Swenie et al. 2018)
H. repando-orientale	TUMH60745 (**T**)	–	AB906683	–	Japan	(Yanaga et al. 2015)
H. repando-orientale	TUMH60743	–	AB906684	–	Japan	(Yanaga et al. 2015)
H. repandum	H6003710 (**T**)	–	NR164553	–	Finland	(Niskanen et al. 2018)
H. roseotangerinum	MHKMU LP Tang 3458 (**T**)	PQ287756	PQ287675	PQ295849	China	(Su et al. 2024)
H. roseotangerinum	MHKMU LP Tang 3458-1	PQ287757	PQ287676	PQ295850	China	(Su et al. 2024)
H. rufescens	H6003708 (**T**)	–	KX388688	–	Finland	(Niskanen et al. 2018)
H. rufescens	HTN7839	–	KX388656	–	Estonia	(Niskanen et al. 2018)
H. slovenicum	LJU-GIS-1338 (**T**)	–	AJ547870	–	Slovenia	(Grebenc et al. 2009)
H. slovenicum	LJU-GIS-1340	–	AJ547884	–	Slovenia	(Grebenc et al. 2009)
H. sp.	wi1A4spel	–	KC679833	–	China	(Cao et al. 2021)
H. sp.	wi8T4spel	–	KC679834	–	China	(Cao et al. 2021)
H. sp.13	HKAS57714	KU612673	KU612617	–	China	(Feng et al. 2016)
H. sp.13	HKAS58838	KU612675	KU612616	–	China	(Feng et al. 2016)
H. sp.2	HKAS92340	KU612661	KU612543	–	China	(Feng et al. 2016)
H. sphæricum	Wei10243 (**T**)	MW979549	MW980563	MW999444	China	(Cao et al. 2021)
H. sphæricum	Wei10300	MW979550	MW980564	MW999445	China	(Cao et al. 2021)
H. sphæricum	Wei10262	MW979551	MW980565	MW999446	China	(Cao et al. 2021)
H. subberkeleyanum	TNSF 19323	–	LC621879	–	Japan	(Sugawara et al. 2022)
H. subberkeleyanum	TUMH63627	–	LC621880	LC622505	Japan	(Sugawara et al. 2022)
H. subconnatum	RAS235 (**T**)	–	MH379930	–	USA	(Swenie et al. 2018)
H. subconnatum	RAS169	–	MH379916	–	USA	(Swenie et al. 2018)
H. submulsicolor	HTN10132 (**T**)	–	KX388682	–	Canada	(Niskanen et al. 2018)
H. subolympicum	F1188765	KU612653	KU612599	–	USA	(Feng et al. 2016)
H. subolympicum	DAOM744368 (**T**)	–	MH174257	–	Canada	(Niskanen et al. 2018)
H. subovoideisporum	H6003707 (**T**)	–	NR158494	–	Finland	(Niskanen et al. 2018)
H. subrufescens	HTN10154 (**T**)	–	KX388649	–	Canada	(Niskanen et al. 2018)
H. subrufescens	F1188749	KU612663	KU612535	–	USA	(Feng et al. 2016)
H. subtilior	RAS180	–	MH379918	–	USA	(Swenie et al. 2018)
H. subtilior	TENN073034 (**T**)	–	NR164029	–	USA	(Swenie et al. 2018)
H. tenuistipitum	IFP 019476 (**T**)	MW979557	MW980576	–	China	(Cao et al. 2021)
H. tenuistipitum	IFP 019477	MW979558	MW980577	–	China	(Cao et al. 2021)
H. tomæense	TUMH64086 (**T**)	–	NR176701	–	Japan	(Sugawara et al. 2022)
H. tottoriense	TUMH64091 (**T**)	–	LC621890	LC622514	Japan	(Sugawara et al. 2022)
H. tottoriense	TUMH64089	–	LC621888	LC622512	Japan	(Sugawara et al. 2022)
H. treui	KA20-0732	ON907772	ON907793	OR220061	Korea	(Niskanen et al. 2018)
H. vagabundum	10782TJB	–	MH379949	–	USA	(Swenie et al. 2018)
H. vagabundum	CLO4985 (**T**)	–	MH379909	–	USA	(Swenie et al. 2018)
H. ventricosum	Yuan14536 (**T**)	MW979547	MW980561	MW999442	China	(Cao et al. 2021)
H. ventricosum	Yuan14601	MW979548	MW980562	MW999443	China	(Cao et al. 2021)
H. vesterholtii	BIO:Fungi:10429 (**T**)	–	HE611084	–	Spain	(Olariaga et al. 2012)
H. vesterholtii	BIO:Fungi:10452	–	HE611085	–	Spain	(Olariaga et al. 2012)
H. washingtonianum	UBCF-32538 (isotype)	–	MF954990	–	Canada	(Cao et al. 2021)
H. zongolicense	GO-2010-142a (**T**)	–	KC152121	–	Mexico	(Niskanen et al. 2018)
Sistotrema muscicola	KHL 11721	–	AJ606040	–	Sweden	(Nilsson et al. 2006)
Sistotrema muscicola	taxon:154757	–	AJ606041	–	Sweden	(Nilsson et al. 2006)

Note: Newly generated sequences in this study are shown in bold; the type specimen is marked by a boldfaced (T).

Results

Phylogenetic analyses

In the concatenated (ITS–nrLSU–*tef*1-α) dataset, 99 samples and 156 sequences underwent phylogenetic analysis. The multiple sequence alignment featured 111 sequences, with 3831 column sites and 1056 distinct patterns, including 3128 (81.65%) constant sites, 125 singleton sites, and 578 (15.09%) parsimony-informative sites. In both the maximum likelihood (ML) phylogenetic analysis and Bayesian inference (BI) analysis, the best-fit partitioned models were selected using the Bayesian Information Criterion (BIC). Specifically, for the maximum likelihood (ML) analysis, the best-fit partitioned models were HKY+F+G4 for ITS, HKY+F+R2 for nrLSU, and TNe+G4 for *tef*1-α. Similarly, for the Bayesian inference (BI) analysis, the best-fit partitioned models were HKY+F+G4 for ITS, HKY+F+I+G4 for nrLSU, and SYM+G4 for *tef*1-α. There was topological consistency between the maximum likelihood (ML) and Bayesian inference (BI) methods, and the BI tree is provided in this study (Figs 1, 2). A total of 20 newly generated sequences from this study, including ten ITS sequences and ten *tef*1-α sequences, were deposited in GenBank.

The phylogenetic tree revealed six major clades, corresponding to six subgenera: *Rufescentia*, *Hydnum*, *Pallida*, *Brevispina*, *Alba* s.l., and *Alba*. The newly generated sequences were divided into five species-level clades with high support values (BPP = 0.98–1; MLBS = 93–100%). Among them, FJAU66576/FJAU66577 (BPP/MLBS = 1/98) were nested within the *H. berkeleyanum* clade and formed a distinct lineage within the subsect. *Rufescentia*; *H. pallidomarginatum* (MLBS = 93), *H. albodentum* (BPP/MLBS = 0.98/100), *H. luteoalbum* (BPP/MLBS = 1/100), and *H. albotomentosum* (BPP = 1, MLBS = 100) each formed a distinct lineage within the subgenus *Pallida*; FJAU66578/FJAU66579 were nested within the *H. pallidomarginatum* clade; *H. albodentum* is closely related to *H. flabellatum*; and *H. luteoalbum* and *H. albotomentosum* form a sister clade (Figs 1, 2).

Taxonomy

Hydnum albodentum **Yonglan Tuo, Bo Zhang & Yu Li, sp. nov.**

Fungal Names: FN 572951

Fig. 3A–G

Etymology. The specific epithet "*albodentum*" refers to the pure white coloration of the fungal spines.

Holotype. CHINA • Anhui Province, Lu'an City, Jinzhai County, Yanzihe Town, 31°18'20"N, 115°55'32"E, Elevation: ca. 752 m. on soil in mixed forests (*Quercus serrata* Thunb. and *Cunninghamia lanceolata* (Lamb.) Hook.), 10 September 2023, Yonglan Tuo FJAU66580. GenBank accession numbers: ITS = PV997562, *tef*1-α = PX026328.

Diagnosis. *H. albodentum* differs from other *Hydnum* species primarily in its medium-sized (7.93–6.78 μm), elliptical spores (Q = 1.13–1.25), and the presence of a white tomentum covering the pileus margin.

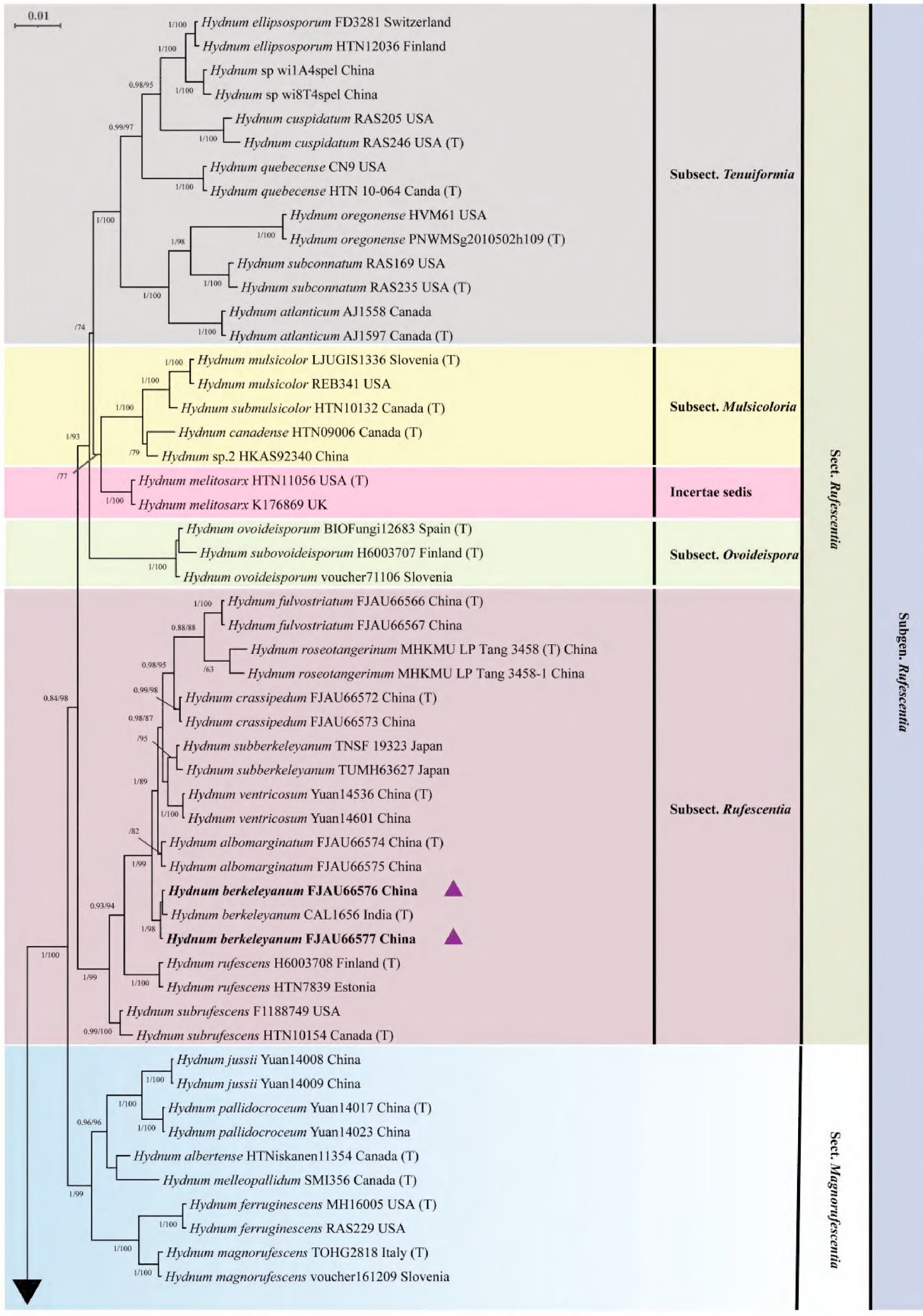
0.01
Hydnum ellipsosporum FD3281 Switzerland
Hydnum ellipsosporum HTN12036 Finland
Hydnum sp wi1A4spel China
Hydnum sp wi8T4spel China
Hydnum cuspidatum RAS205 USA
Hydnum cuspidatum RAS246 USA (T)
Hydnum quebecense CN9 USA
Hydnum quebecense HTN 10-064 Canda (T)
Hydnum oregonense HVM61 USA
Hydnum oregonense PNWMSg2010502h109 (T)
Hydnum subconnatum RAS169 USA
Hydnum subconnatum RAS235 USA (T)
Hydnum atlanticum AJ1558 Canada
Hydnum atlanticum AJ1597 Canada (T)
Subsect. Tenuiformia
Hydnum mulsicolor LJUGIS1336 Slovenia (T)
Hydnum mulsicolor REB341 USA
Hydnum submulsicolor HTN10132 Canada (T)
Hydnum canadense HTN09006 Canada (T)
Hydnum sp.2 HKAS92340 China
Subsect. Mulsicoloria
Hydnum melitosarx HTN11056 USA (T)
Hydnum melitosarx K176869 UK
Incertae sedis
Hydnum ovoideisporum BIOFungi12683 Spain (T)
Hydnum subovoideisporum H6003707 Finland (T)
Hydnum ovoideisporum voucher71106 Slovenia
Subsect. Ovoideispora
Hydnum fulvostriatum FJAU66566 China (T)
Hydnum fulvostriatum FJAU66567 China
Hydnum roseotangerinum MHKMU LP Tang 3458 (T) China
Hydnum roseotangerinum MHKMU LP Tang 3458-1 China
Hydnum crassipedum FJAU66572 China (T)
Hydnum crassipedum FJAU66573 China
Hydnum subberkeleyanum TNSF 19323 Japan
Hydnum subberkeleyanum TUMH63627 Japan
Hydnum ventricosum Yuan14536 China (T)
Hydnum ventricosum Yuan14601 China
Hydnum albomarginatum FJAU66574 China (T)
Hydnum albomarginatum FJAU66575 China
Hydnum berkeleyanum FJAU66576 China
Hydnum berkeleyanum CAL1656 India (T)
Hydnum berkeleyanum FJAU66577 China
Hydnum rufescens H6003708 Finland (T)
Hydnum rufescens HTN7839 Estonia
Hydnum subrufescens F1188749 USA
Hydnum subrufescens HTN10154 Canada (T)
Subsect. Rufescentia
Hydnum jussii Yuan14008 China
Hydnum jussii Yuan14009 China
Hydnum pallidocroceum Yuan14017 China (T)
Hydnum pallidocroceum Yuan14023 China
Hydnum albertense HTNiskanen11354 Canada (T)
Hydnum melleopallidum SMI356 Canada (T)
Hydnum ferruginescens MH16005 USA (T)
Hydnum ferruginescens RAS229 USA
Hydnum magnorufescens TOHG2818 Italy (T)
Hydnum magnorufescens voucher161209 Slovenia
Sect. Magnorufescentia
Sect. Rufescentia
Subgen. Rufescentia

Figure 1. Phylogenetic tree inferred from Bayesian inference (BI) based on the combined dataset (ITS–nrLSU–*tef*1-α). The values on the nodes represent Bayesian posterior probability (left, BPP ≥ 0.95) and maximum likelihood bootstrap support (right, MLBS ≥ 75%), respectively. Novel sequences generated in this study appear in boldface type; holotype specimens are marked with (T); new taxa are marked with filled pentagrams (Purple star); and newly recorded taxa are marked with solid triangles (Purple up-pointing triangle).

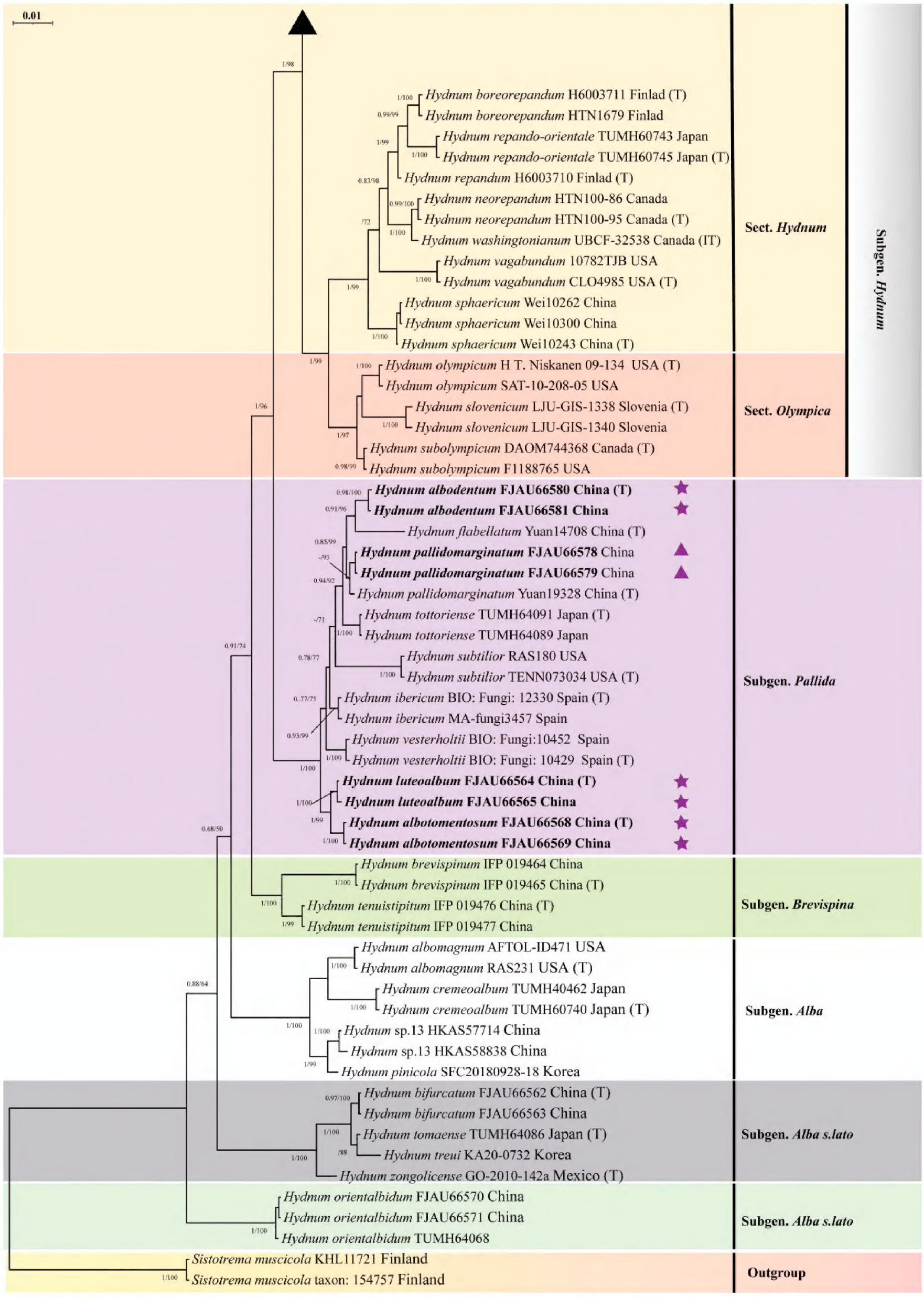
0.01
Hydnum boreorepandum H6003711 Finlad (T)
Hydnum boreorepandum HTN1679 Finlad
Hydnum repando-orientale TUMH60743 Japan
Hydnum repando-orientale TUMH60745 Japan (T)
Hydnum repandum H6003710 Finlad (T)
Hydnum neorepandum HTN100-86 Canada
Hydnum neorepandum HTN100-95 Canada (T)
Hydnum washingtonianum UBCF-32538 Canada (IT)
Hydnum vagabundum 10782TJB USA
Hydnum vagabundum CLO4985 USA (T)
Hydnum sphaericum Wei10262 China
Hydnum sphaericum Wei10300 China
Hydnum sphaericum Wei10243 China (T)
Sect. Hydnum
Subgen. Hydnum
Hydnum olympicum H T. Niskanen 09-134 USA (T)
Hydnum olympicum SAT-10-208-05 USA
Hydnum slovenicum LJU-GIS-1338 Slovenia (T)
Hydnum slovenicum LJU-GIS-1340 Slovenia
Hydnum subolympicum DAOM744368 Canada (T)
Hydnum subolympicum F1188765 USA
Sect. Olympica
Hydnum albodentum FJAU66580 China (T)
Hydnum albodentum FJAU66581 China
Hydnum flabellatum Yuan14708 China (T)
Hydnum pallidomarginatum FJAU66578 China
Hydnum pallidomarginatum FJAU66579 China
Hydnum pallidomarginatum Yuan19328 China (T)
Hydnum tottoriense TUMH64091 Japan (T)
Hydnum tottoriense TUMH64089 Japan
Hydnum subtilior RAS180 USA
Hydnum subtilior TENN073034 USA (T)
Hydnum ibericum BIO: Fungi: 12330 Spain (T)
Hydnum ibericum MA-fungi3457 Spain
Hydnum vesterholtii BIO: Fungi:10452 Spain
Hydnum vesterholtii BIO: Fungi: 10429 Spain (T)
Hydnum luteoalbum FJAU66564 China (T)
Hydnum luteoalbum FJAU66565 China
Hydnum albotomentosum FJAU66568 China (T)
Hydnum albotomentosum FJAU66569 China
Subgen. Pallida
Hydnum brevispinum IFP 019464 China
Hydnum brevispinum IFP 019465 China (T)
Hydnum tenuistipitum IFP 019476 China (T)
Hydnum tenuistipitum IFP 019477 China
Subgen. Brevispina
Hydnum albomagnum AFTOL-ID471 USA
Hydnum albomagnum RAS231 USA (T)
Hydnum cremeoalbum TUMH40462 Japan
Hydnum cremeoalbum TUMH60740 Japan (T)
Hydnum sp.13 HKAS57714 China
Hydnum sp.13 HKAS58838 China
Hydnum pinicola SFC20180928-18 Korea
Subgen. Alba
Hydnum bifurcatum FJAU66562 China (T)
Hydnum bifurcatum FJAU66563 China
Hydnum tomaense TUMH64086 Japan (T)
Hydnum treui KA20-0732 Korea
Hydnum zongolicense GO-2010-142a Mexico (T)
Subgen. Alba s.lato
Hydnum orientalbidum FJAU66570 China
Hydnum orientalbidum FJAU66571 China
Hydnum orientalbidum TUMH64068
Subgen. Alba s.lato
Sistotrema muscicola KHL11721 Finland
Sistotrema muscicola taxon: 154757 Finland
Outgroup

Figure 2. Phylogenetic tree inferred from Bayesian inference (BI) based on the combined dataset (ITS–nrLSU–*tef*1-α). The values on the nodes represent Bayesian posterior probability (left, BPP ≥ 0.95) and maximum likelihood bootstrap support (right, MLBS ≥ 75%), respectively. Novel sequences generated in this study appear in boldface type; holotype specimens are marked with (T); new taxa are marked with filled pentagrams (Purple star); and newly recorded taxa are marked with solid triangles (Purple up-pointing triangle).

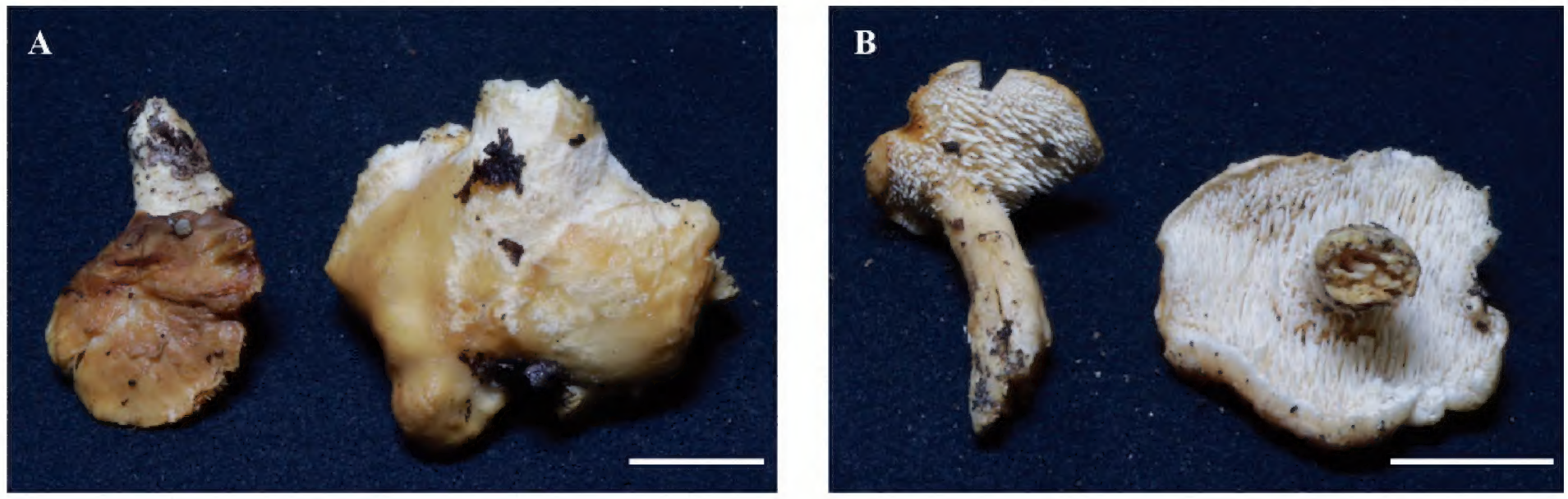

Figure 3. Macroscopic and microscopic features of *H. albodentum* (FJAU66580, holotype). **A–D.** Basidiomata; **E.** Hymenium and subhymenium; **F.** Basidiospores; **G.** Pileipellis. Scale bars: 2 cm (**A–D**); 10 μm (**E–G**).

Description. Basidiocarps small, solitary, 25.5–40.5 mm in height, fleshy when fresh. Pileus 27.5–55.5 mm wide, brownish orange to light brown (6C6–6D7), convex to plano-convex when mature, surface smooth, margin incurved and covered with white (4A1) tomentum. Context 2.5–4.5 mm thick, white (4A1). Hymenophore hydnoid, spines fleshy, non-decurrent, conical, sparse, 1–2 spines/mm^2; surface white (4A1), 3.0–7.5 mm long, 0.5–1.5 mm diameter. Stipe cylindrical, 21.5–35.0 × 8.5–10.5 mm, solid, central, equal to slightly enlarged at the base, white to light brown (4A1–6C6), covered with white basal mycelium, brownish orange when handled. Odor mild or fruity.

Basidiospores (7.0) 8.0–8.5 (9.0) × (5.5) 6.0–7.0 (8.0) μm, av. L = 7.93 μm, av. W = 6.78 μm, Q = (1.0) 1.13–1.25 (1.33), av. Q = 1.17, ellipsoid, thin-walled, smooth, hyaline in 3% KOH, some with granular contents; hilar appendix 0.5–1.0 μm long. Basidia (30.0) 32.5–45.0 (55.0) × (8.0) 9.0–10.0 (12.0) μm, subcylindric, some with granular contents and hyaline oily droplets; sterigmata 2–5, 4.0–5.0 × 0.5–1.0 μm, conical, thin-walled, smooth. Basidioles 25.0–32.0 × 7.0–9.0 μm, numerous, smaller than basidia, some with granular contents. Subhymenium trama filamentous, hyphae 2.5–3.0 μm wide, thin-walled, hyaline in 3% KOH. Hyphae of spines 5.0–7.0 μm, thin-walled, apex cylindrical. Pileipellis

composed of cylindrical hyphae, slightly interwoven; terminal elements cylindrical at apex, cells 65.5–105.5 × 8.5–10.0 µm. Stipitipellis composed of cylindrical hyphae, slightly interwoven, 6.0–7.5 µm wide, terminal elements rounded at apex. Clamp connections present.

Habitat and distribution. The species occurs solitarily in a mixed forest (*Q. serrata* and *C. lanceolata*) within the buffer zone of Tianma National Nature Reserve, China (ca. 700–800 m, subtropical monsoon climate). The forest is subject to human disturbance (grazing, thinning, and proximity to villages at approximately 1.5–2.5 km). The specimen was collected at a distance of 45.6 cm from a *C. lanceolata* tree (DBH: 23.6 cm) and at a distance of 85.6 cm from a *Q. serrata* tree (DBH: 15.6 cm). Soil temperature was 12.1 °C, soil volumetric water content was 25.3%, soil pH was 5.9, air temperature was 24.2 °C, and relative humidity was 88.5%. Soil temperature, moisture content, and pH were measured at the time of sample collection; air temperature and humidity were monitored over the long term within the sample plot (measurements were taken at 10-minute intervals; these data are mean values calculated over the 3 days preceding and following sample collection).

Additional specimens examined. CHINA • Anhui Province, Lu'an City, Jinzhai County, 31°18'41"N, 115°55'01"E, Elevation: ca. 742 m. on soil in *Q. serrata* and *C. lanceolata* mix forests, 10 September 2023, Yonglan Tuo FJAU66581. GenBank accession numbers: ITS = PV997563, *tef*1-α = PX026329.

Notes. Morphologically, *H. albodentum* is similar to *H. pallidomarginatum* in having small basidiocarps (27.5–55.5 mm *vs.* 20.0–35.0 mm), but it is distinct from *H. pallidomarginatum* in having smaller basidiospores (7.93 × 6.78 µm *vs.* 8.75 × 6.99 µm) and a brownish orange to light brown pileus.

In the phylogenetic tree, the sequences of *H. albodentum* cluster together, forming a distinct lineage and a sister clade with *H. flabellatum* within subgenus *Pallida*.

Hydnum albotomentosum **Yonglan Tuo, Bo Zhang & Yu Li, sp. nov.**

Fungal Names: FN 572699

Fig. 4A–F

Etymology. The specific epithet "*albotomentosum*" refers to the white tomentum covering the pileus and stipe of immature basidiocarps.

Holotype. CHINA • Anhui Province, Lu'an City, Tianma National Nature Reserve, 31°13'10"N, 115°46'53"E, Elevation: ca. 817 m. on soil in mixed forests (*Quercus variabilis* Blume and *Pinus hwangshanensis* W.Y.Hsia), 8 August 2023, Yonglan Tuo FJAU66568. GenBank accession numbers: ITS = PV329851, *tef*1-α = PP357256.

Diagnosis. *H. albotomentosum* differs from other *Hydnum* species in its relatively small basidiocarps, short spines (0.5–2.0 mm), and the presence of a white tomentum covering the pileus surface when immature, which disappears upon maturity.

Description. Basidiocarps small, solitary, 22.0–30.0 mm in height, fleshy when fresh. Pileus 16.5–29.5 mm wide, pale orange to deep orange (5A3–4A8), convex to plano-convex when mature, margin incurved, surface covered with white (4A1) tomentum when immature, tomentum disappearing upon maturity.

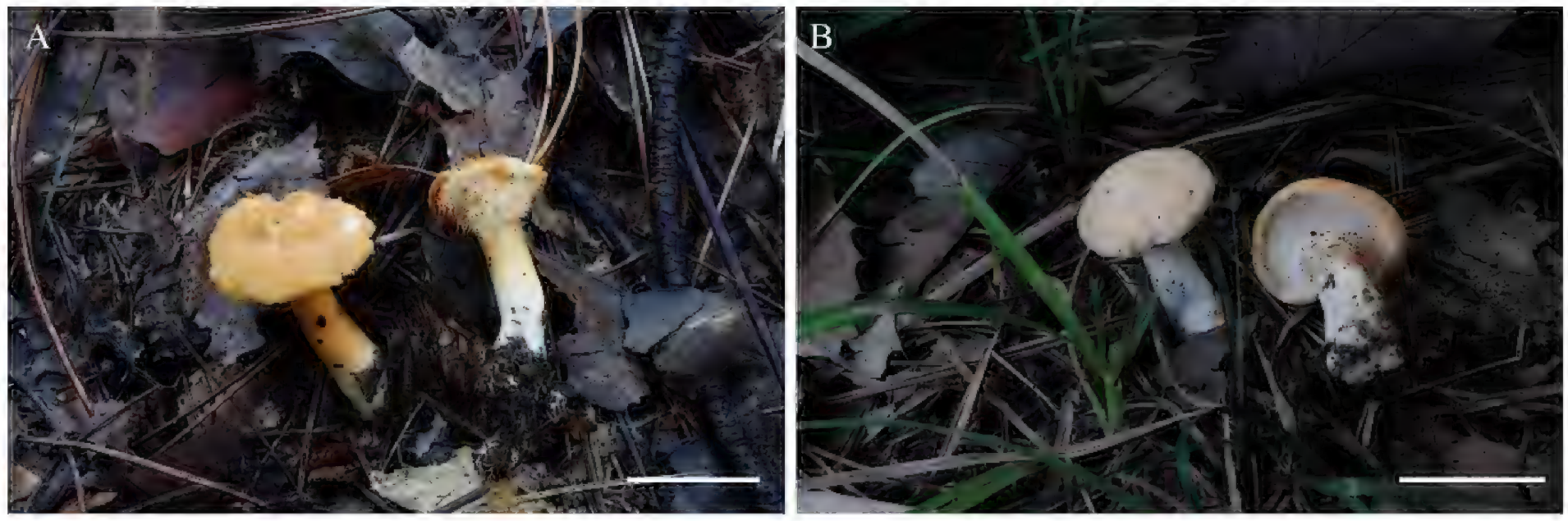

Figure 4. Macroscopic and microscopic features of *H. albotomentosum* (FJAU66568, holotype). **A–C.** Basidiomata; **D.** Hymenium and subhymenium; **E.** Basidiospores; **F.** Pileipellis. Scale bars: 2 cm (**A–C**); 10 μm (**D–F**).

Context 2.5–5.0 mm thick, white (4A1). Hymenophore hydnoid, spines fleshy, non-decurrent, conical, sparse, 1–2 spines/mm^2; surface white to yellowish white (4A1–4A2), 0.5–2.0 mm long, 0.25–0.5 mm diameter. Stipe cylindrical, 20.0–30.0 × 7.0–10.0 mm, solid, central, equal to slightly enlarged at the base, white to deep orange (4A1–4A8), covered with a large amount of white basal mycelium; Stipe at first whitish, staining pale brownish orange when handled. Odor mild or fruity.

Basidiospores (6.0) 7.0–8.0 (8.5) × (5.5) 6.5–7.0 (8.0) μm, av. L = 7.11 μm, av. W = 6.72 μm, Q = 1.0–1.14, av. Q = 1.06, globose to subglobose, thin-walled, smooth, hyaline in 3% KOH, some with granular contents; hilar appendix 0.5–1.0 μm long. Basidia (33.0) 36.0–42.0 (46.0) × (7.5) 9.0–10.0 (12.0) μm, clavate

to suburniform, some with granular contents and hyaline oily droplets; sterigmata 2–4, 4.0–6.0 × 1.0–2.0 µm, conical, thin-walled, smooth. Basidioles (28.0) 30.0–38.0 (42.0) × (6.0) 8.0–10.0 (12.0) µm, numerous, smaller than basidia, some with granular contents. Subhymenium trama filamentous, hyphae 3.0–4.0 µm wide, thin-walled, hyaline in 3% KOH. Hyphae of spines 6.5–7.0 µm, thin-walled, apex cylindrical. Pileipellis composed of cylindrical hyphae, subparallel to slightly interwoven; terminal elements cylindrical at apex, cells 56.0–105.0 × 5.5–7.0 µm. Stipitipellis composed of cylindrical hyphae, slightly interwoven, 4.0–6.0 µm wide, terminal elements rounded at apex. Clamp connections present.

Habitat and distribution. The species occurs solitarily in a mixed forest (*Q. variabilis* and *P. hwangshanensis*) within the buffer zone of Tianma National Nature Reserve, China (ca. 800–900 m, subtropical monsoon climate). The forest is subject to human disturbance (grazing, thinning, and proximity to villages and towns at approximately 0.5–3.5 km). Specimens were collected at a distance of 139.5 cm from a *P. hwangshanensis* tree (DBH: 50.6 cm) and at a distance of 85.6 cm from a *Q. variabilis* tree (DBH: 25.6 cm). Soil temperature was 24.1 °C, soil volumetric water content was 24.2%, soil pH was 5.2, air temperature was 25.6 °C, and relative humidity was 85.6%. Soil temperature, moisture content, and pH were measured at the time of sample collection; air temperature and humidity were monitored over the long term within the sample plot (measurements were taken at 10-minute intervals; these data are mean values calculated over the 3 days preceding and following sample collection).

Additional specimens examined. CHINA • Anhui Province, Lu'an City, Tianma National Nature Reserve, 31°13'14"N, 115°46'55"E, Elevation: ca. 856 m. on soil in *Q. variabilis* and *P. hwangshanensis* mixed forests, 17 July 2023, Yonglan Tuo FJAU66569. GenBank accession numbers: ITS = PV329852, *tef*1-α = PP357257.

Notes. Morphologically, *H. albotomentosum* is similar to *H. ibericum* in having a white to cream pileus and small basidiocarps (16.5–29.5 mm *vs.* 22.0–30.0 mm), but it is distinct from *H. ibericum* in having smaller basidiospores (7.11 × 6.72 µm *vs.* 8.2 × 6.4 µm).

In the phylogenetic tree, the sequences of *H. albotomentosum* form a distinct lineage and group within a large subclade with strong support (100% ML and 1.00 BPP) together with *H. vesterholtii*, *H. ibericum*, *H. subtilior*, *H. tottoriense*, *H. flabellatum*, *H. pallidomarginatum*, and *H. luteoalbum*. Based on the morphological characteristics described above and the phylogenetic results, *H. albotomentosum* should be classified as a member of subgenus *Pallida*.

Hydnum berkeleyanum K. Das, Hembrom, Baghela & Vizzini, 2018

Fig. 5A–E

Habitat and distribution. The species grows gregariously in a *Q. serrata* forest within the core zone of Tianma National Nature Reserve, China (ca. 1000–1100 m, subtropical monsoon climate). It is currently known from India, Pakistan, Anhui Province, and Yunnan Province in China. The specimen was collected at a distance of 105.6 cm from a *Q. serrata* tree (DBH: 56.8 cm). Soil temperature was 20.6 °C, soil volumetric water content was 17.5%, soil pH was 5.9, air temperature was 23.2 °C, and relative humidity was 91.2%. Soil temperature, moisture content, and pH were measured at the time of sample collection;

Figure 5. Macroscopic and microscopic features of *H. berkeleyanum*. **A, B.** Basidiomata; **C.** Hymenium and subhymenium; **D.** Basidiospores; **E.** Pileipellis. Scale bars: 2 cm (**A, B**); 10 μm (**C–E**).

air temperature and humidity were monitored over the long term within the sample plot (measurements were taken at 10-minute intervals; these data are mean values calculated over the 3 days preceding and following sample collection).

Specimens examined. CHINA • Anhui Province, Lu'an City, Tianma National Nature Reserve, 31°15'20"N, 115°42'09"E, Elevation: ca. 1049 m, 23 July 2023, Yonglan Tuo (FJAU66576), GenBank accession numbers: ITS = PV875855, *tef*1-α = PV889364); • Anhui Province, Lu'an City, Tianma National Nature Reserve, 31°15'21"N, 115°42'07"E, Elevation: ca. 1052 m, 16 July 2023, Yonglan Tuo (FJAU66577), GenBank accession numbers: ITS = PV875856, *tef*1-α = PV889365.

Notes. No major differences were found between our specimens and the type; however, the habitat of our specimens (*Q. serrata* forest) differs from that in the original description (mixed forest). Phylogenetic analyses based on multi-marker datasets indicate that the two specimens from Anhui are well nested within the *H. berkeleyanum* clade.

Hydnum luteoalbum **YonglanTuo, Bo Zhang & Yu Li, sp. nov.**

Fungal Names: FN 572683

Fig. 6A–F

Etymology. The specific epithet "*luteoalbum*" refers to the yellowish-white color of the entire basidiocarp.

Holotype. CHINA • Anhui Province, Lu'an City, Tianma National Nature Reserve, 31°15'43"N, 115°41'41"E, Elevation: ca. 1207 m. on soil in *Quercus serrata* Thunb. forest, 4 August 2023, Yonglan Tuo FJAU66564. GenBank accession numbers: ITS: PV329847, *tef*1-α: PP357254.

Diagnosis. *H. luteoalbum* differs from other species of *Hydnum* by its ensiform-dagger spines, white pileus, and smaller basidiospores (7.0–7.5 × 6.0–6.5 µm).

Description. Basidiocarps small to medium, solitary, 25.0–30.0 mm in height. Pileus 25.0–60.5 mm wide, white to yellowish white (4A1–4A2), round to irregular, shallowly depressed in the center, discoloration not observed; margin incurved, azonate, white (4A1) tomentum; pileus context 2.0–4.5 mm thick. Hymenophore hydnoid, spines non-decurrent, ensiform, slightly sparse, 1–2 spines/mm^2, white to yellowish white (4A1–4A2), 5.0–10.0 mm long, 0.5–1.5 mm diameter. Stipe 20.0–35.0 × 7.0–15.0 mm, central to slightly eccentric, solid, surface covered with white (4A1) tomentum. Odor mild or fruity.

Basidiospores (6.0) 7.0–7.5 (8.0) × (5.5) 6.0–6.5 (7.0) µm, av. L = 7.08 µm, av. W = 6.10 µm, Q = (1.00) 1.08–1.17 (1.33), av. Q = 1.16, broadly ellipsoid, thin-walled, smooth, hyaline in 3% KOH, some with granular contents, inamyloid, hilar appendix 0.5–1.0 µm long. Basidia (35.0) 36.0–50.0 (55.0) × (7.0) 8.0–10.0 (11.0) µm, clavate to suburniform, some with granular contents, sterigmata 2–4, 4.0–6.5 × 1.0–2.0 µm, conical, thin-walled, smooth. Basidioles (25.0) 30.0–40.0 (50) × (6.0) 7.0–10.0 (11.0) µm, smaller than basidia, some with granular contents. Subhymenium trama filamentous, hyphae 4.0–5.0 µm wide, thin-walled, hyaline in 3% KOH. Hyphae of spines 7.0–8.0 µm, thin-walled, apex cylindrical. Pileipellis composed of cylindrical hyphae, slightly interwoven, terminal elements cylindrical at apex, cells 60.0–125.0 × 7.0–11.0 µm. Stipitipellis composed of cylindrical hyphae, slightly interwoven, 6.0–14.0 µm wide, terminal elements dilated at apex. Clamp connections present.

Habitat and distribution. The species occurs solitarily in a *Q. serrata* forest within the core zone of Tianma National Nature Reserve, China (ca. 1100–1300 m, subtropical monsoon climate), with minimal human disturbance. Specimens were collected at a distance of 42.5 cm from a *Q. serrata* tree, with a diameter at breast height (DBH: 18.14 cm). Soil temperature was 22.5 °C, soil volumetric water content was 20.5%, soil pH was 5.8, air temperature was 24.2 °C, and relative humidity was 90.1%. Soil temperature, moisture content, and pH were measured at the time of sample collection; air temperature and humidity were monitored over the long term within the sample plot (measurements were taken at 10-minute intervals; these data are mean values calculated over the 3 days preceding and following sample collection).

Additional specimens examined. CHINA • Anhui Province, Lu'an City, Tianma National Nature Reserve, 31°15'40"N, 115°41'46"E, Elevation: ca. 1193 m. on soil in *Q. serrata* Thunb. forest, 4 August 2023, Yonglan Tuo FJAU66565. GenBank accession numbers: ITS = PV329848, *tef*1-α = PP357255.

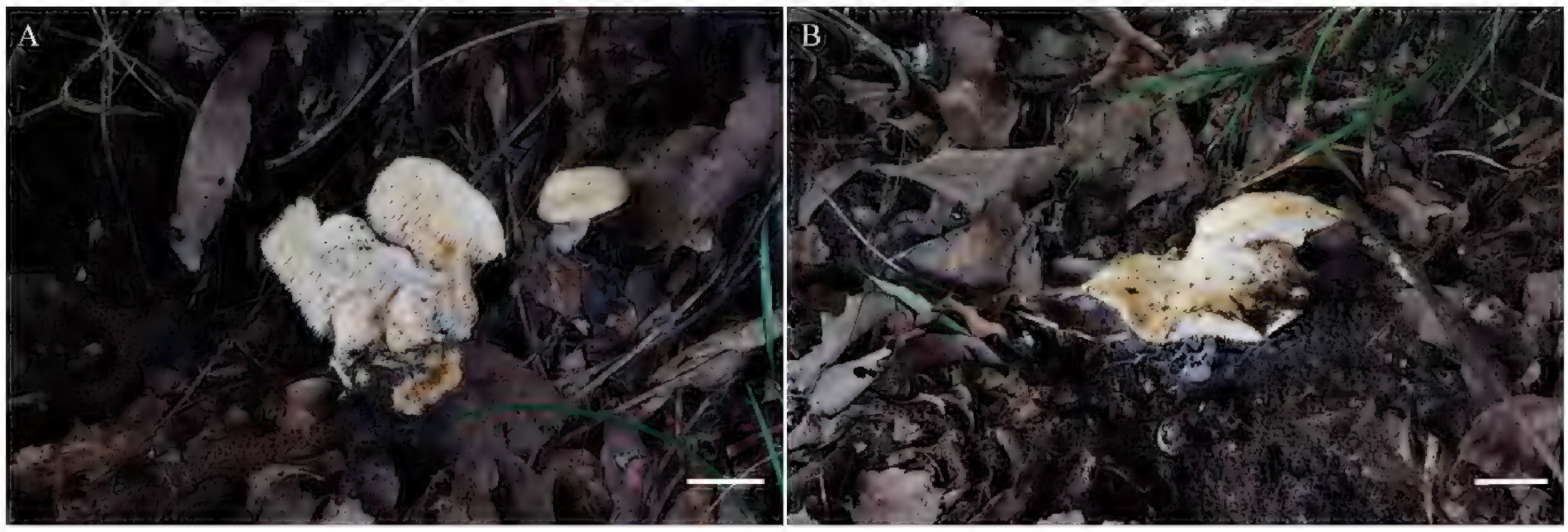

Figure 6. Macroscopic and microscopic features of *H. luteoalbum* (FJAU66564, holotype). **A–C.** Basidiomata; **D.** Hymenium and subhymenium; **E.** Basidiospores; **F.** Pileipellis. Scale bars: 2 cm (**A–C**); 10 μm (**D–F**).

Notes. Morphologically, *H. luteoalbum* has medium-sized basidiocarps and is similar to *H. flavidocanum* in pileus and stipe color, but it has smaller basidiospores (7.08 × 6.10 μm *vs.* 9.81 × 9.03 μm) and smaller basidia (36.0–44.0 × 8.0–10.0 μm *vs.* 45.0–82.0 × 10.0–14.0 μm).

Phylogenetic analysis indicates that *H. luteoalbum* forms a distinct lineage and forms a sister branch to *H. albotomentosum*. Based on the above morphological characters and phylogenetic results, *H. luteoalbum* is easily distinguishable from other species of *Hydnum* and should be classified in subgenus *Pallida*.

***Hydnum pallidomarginatum* T. Cao & H.S. Yuan, 2021**
Fig. 7A–E

Habitat and distribution. The species grows gregariously in a *Q. serrata* forest within the core zone of Tianma National Nature Reserve, China (ca. 900–1000 m, subtropical monsoon climate). It is currently documented in Anhui Province, Yunnan Province, Heilongjiang Province, and Liaoning Province in China. The specimen was collected at a distance of 10.6 cm from a *Q. serrata* tree (DBH: 36.2 cm). Soil temperature was 19.8 °C, soil volumetric water content was 23.2%, soil pH was 6.2, air temperature was 22.0 °C, and relative humidity was 92.5%. Soil temperature, moisture content, and pH were measured

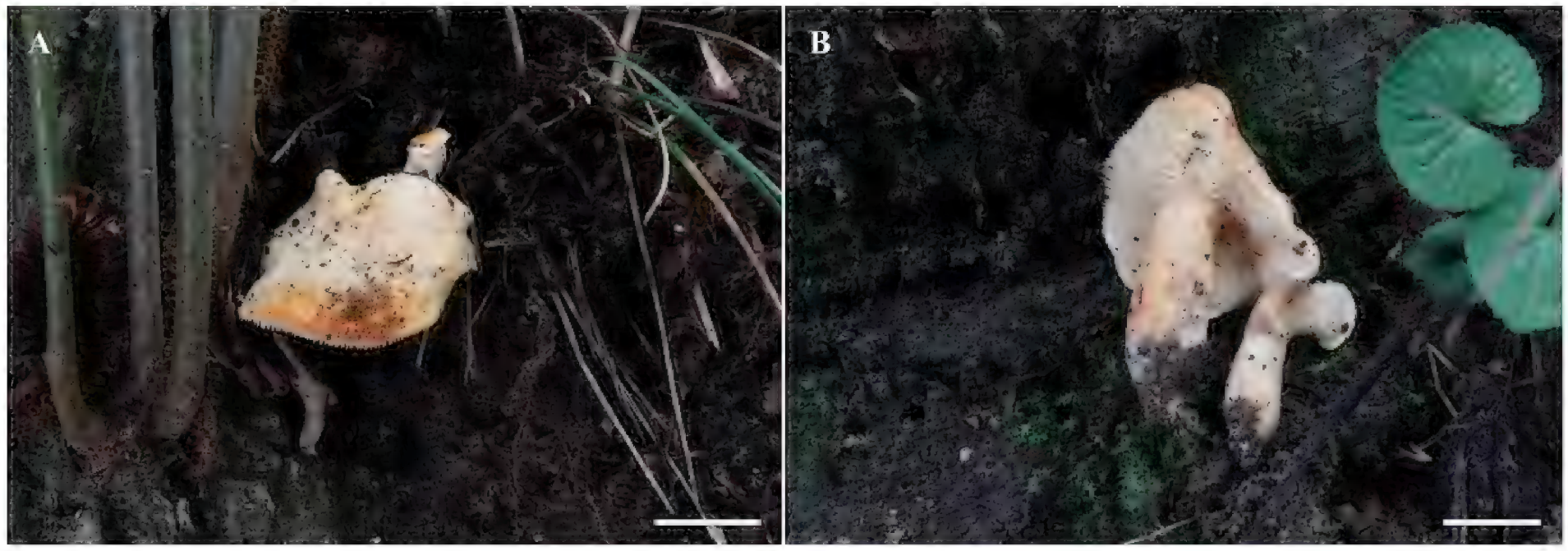

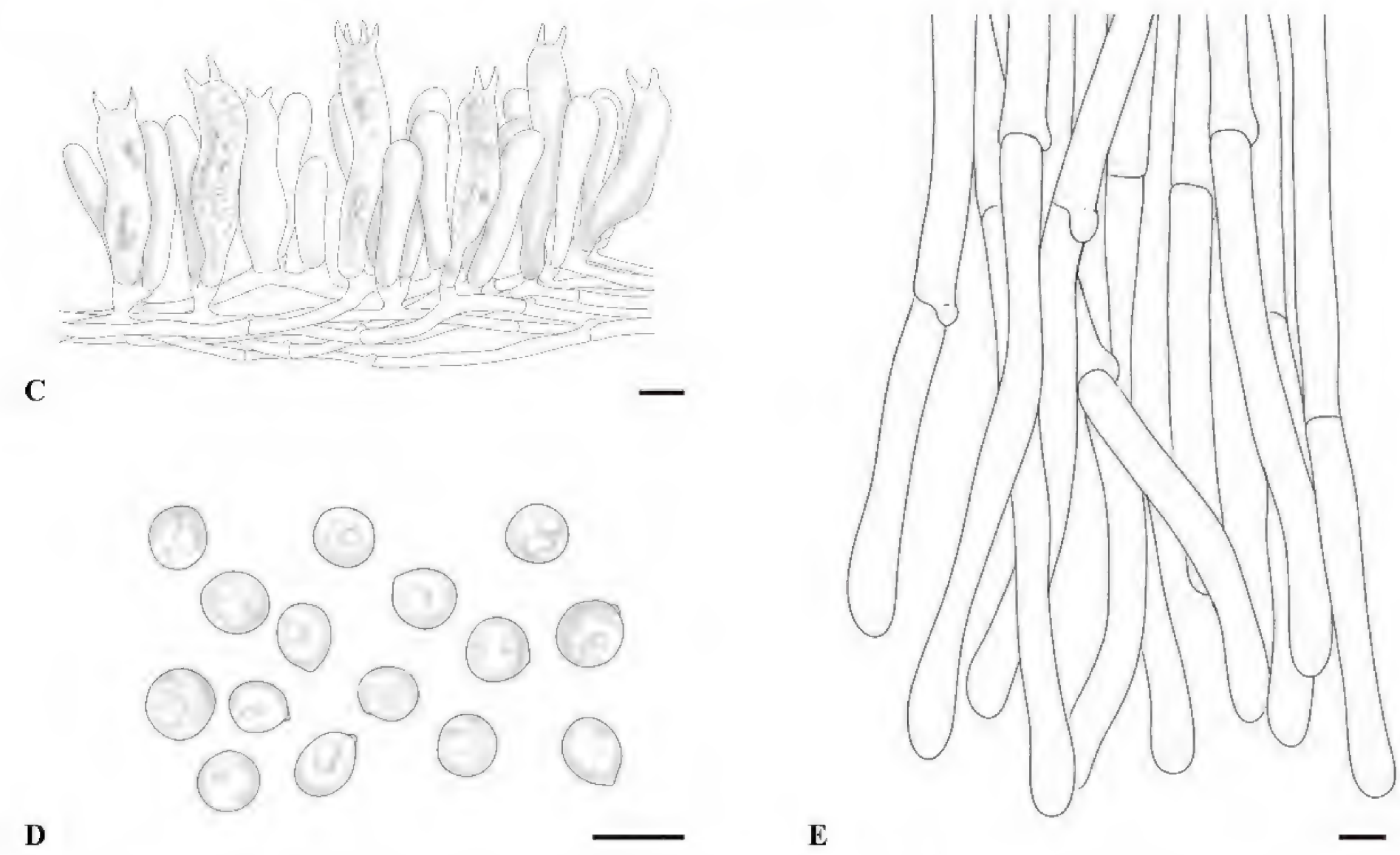

Figure 7. Macroscopic and microscopic features of *H. pallidomarginatum*. **A, B.** Basidiomata; **C.** Hymenium and subhymenium; **D.** Basidiospores; **E.** Pileipellis. Scale bars: 2 cm (**A, B**); 10 μm (**C–E**).

at the time of sample collection; air temperature and humidity were monitored over the long term within the sample plot (measurements were taken at 10-minute intervals; these data are mean values calculated over the 3 days preceding and following sample collection).

Specimens examined. CHINA • Anhui Province, Lu'an City, Tianma National Nature Reserve, 31°15'14"N, 115°42'10"E, Elevation: ca. 960 m, 11 October 2023, Yonglan Tuo (FJAU66578), GenBank accession numbers: ITS = PV875857, *tef*1-α = PV889366. • Anhui Province, Lu'an City, Tianma National Nature Reserve, 31°15'09"N, 115°42'13"E, Elevation: ca. 954 m, 12 October 2023, Yonglan Tuo (FJAU66579), GenBank accession numbers: ITS = PV875858, *tef*1-α = PV889367.

Notes. *H. pallidomarginatum* is characterized by its white to yellowish-white pileus, 2–4 sterigmata, and globose to subglobose basidiospores. It was described from Yunnan Province, China. We examined collections from Yunnan and several DNA sequences from China annotated as *H. pallidomarginatum* in the database. No major differences were found between our specimens and the holotype, except for the color of the pileus. The multi-marker phylogenetic analyses revealed that the two Chinese *H. pallidomarginatum* specimens form a monophyletic cluster within *H. pallidomarginatum*.

Key to Species of *Hydnum* in China

1	Basidiomata more or less white to cream yellow	**2**
–	Basidiomata yellow to orange	**11**
2	Pileus white	**3**
–	Pileus cream yellow	**7**
3	Pileus ≤ 30 mm wide	***H. flavidocanum***
–	Pileus ≥ 30 mm wide	**4**
4	Habitat in broad-leaved forests	**5**
–	Habitat in *Fagaceæ* forests	**6**
5	Pileus ≥ 60 mm wide	***H. cremeoalbum***
–	Pileus < 60 mm wide	***H. orientalbidum***
6	Basidiospores ≤ 5 µm long on average	***H. minus***
–	Basidiospores > 5 µm long on average	***H. treui***
7	Pileus > 60 mm wide	**8**
–	Pileus ≤ 60 mm wide	**9**
8	Habitat in broad-leaved forests	***H. roseoalbum***
–	Habitat in *Quercus mongolica* forests	***H. bifurcatum***
9	Spines ≤ 3 mm long	**10**
–	Spines > 3 mm long	***H. albomagnum***
10	Spines pale orange	***H. pinicola***
–	Spines cream yellow	***H. minum***
11	Basidiomata yellowish-white	**12**
–	Basidiomata orange	**19**
12	Basidiospores < 6 µm long on average	**13**
–	Basidiospores > 6 µm long on average	**14**
13	Habitat in angiosperm forests	***H. brevispinum***
–	Habitat in mixed forests	***H. microcarpum***
14	Basidiospores < 7.5 µm long on average	**15**
–	Basidiospores > 7.5 µm long on average	**18**

15 Pileus > 40 mm wide ..... ***H. fulvostriatum***
– Pileus < 40 mm wide **16**
16 Spines > 3 mm long ..... ***H. luteoalbum***
– Spines ≤ 3 mm long **17**
17 Habitat in September ..... ***H. tenuistipitum***
– Habitat in August ..... ***H. albotomentosum***
18 Habitat in *Q. variabilis* forests ..... ***H. crassipedum***
– Habitat in *Q. serrata* forests ..... ***H. albomarginatum***
19 Basidiospores 7–8 µm long on average **20**
– Basidiospores > 8 µm long on average **22**
20 Pileus ≥ 60 mm wide ..... ***H. jussii***
– Pileus < 60 mm wide **21**
21 Habitat in *Fagaceæ* forests ..... ***H. erectum***
– Habitat in *Q. serrata* and *C. lanceolata* forests ..... ***H. albodentum***
22 Basidiospores 8–9 µm long on average **23**
– Basidiospores > 9 µm long on average **30**
23 Spines white **24**
– Spines orange-white or cream-yellow **25**
24 Spines ≤ 3 mm long ..... ***H. sphaericum***
– Spines ≥ 3 mm long ..... ***H. sinorepandum***
25 Spines cream-yellow ..... ***H. cremeum***
– Spines orange-white to brownish-orange **26**
26 Basidiospores 8.1–8.5 µm long on average **27**
– Basidiospores > 8.5 µm long on average **29**
27 Spines < 2 mm long ..... ***H. vesterholtii***
– Spines > 2 mm long **28**
28 Habitat in angiosperm forests ..... ***H. tangerinum***
– Habitat in *Q. serrata* forest ..... ***H. berkeleyanum***
29 Basidiospores Q < 1.1. ..... ***H. ventricosum***
– Basidiospores Q > 1.1 ..... ***H. pallidomarginatum***
30 Pileus < 50 mm wide **31**
– Pileus > 50 mm wide ..... ***H. roseotangerinum***
31 Spines orange-white to pale-orange **32**
– Spines light-yellow to pale-orange **34**
32 Pileus ≥ 30 mm wide ..... ***H. flabellatum***
– Pileus ≤ 30 mm wide **33**
33 Basidiospores > 9.5 µm long on average ..... ***H. longibasidium***
– Basidiospores < 9.5 µm long on average ..... ***H. longipes***
34 Basidiospores Q > 1.3 ..... ***H. pallidocroceum***
– Basidiospores Q < 1.3 ..... **35**
35 Pileus ≤ 40 mm wide ..... ***H. melitosarx***
– Pileus > 40 mm wide ..... ***H. flavoquamosum***

Discussion

Through a comprehensive analysis integrating morphological and molecular methods, we identified and described three novel species (*H. luteoalbum*, *H. albodentum*, and *H. albotomentosum*) and two newly recorded species from the Dabie Mountains (*H. berkeleyanum* and *H. pallidomarginatum*). Morphological

observations revealed significant differences between *H. luteoalbum*, *H. albodentum*, *H. albotomentosum*, and other *Hydnum* species in key taxonomically informative characteristics, such as pileus color, size, and basidiospore dimensions. Phylogenetic analyses further confirmed that these three species form distinct monophyletic clades, indicating pronounced genetic divergence. In contrast, *H. berkeleyanum* and *H. pallidomarginatum* align with previous taxonomic findings, including both morphological descriptions and phylogenetic placements (Cao et al. 2021; Su et al. 2024).

H. luteoalbum, *H. albodentum*, *H. albotomentosum*, and *H. pallidomarginatum* are characterized by small to medium-sized basidiomata, with pilei ranging in color from white to orange and stipes that are initially white (turning orange upon treatment), which is consistent with the taxonomic criteria of *Hydnum* subgenus *Pallida* (Niskanen et al. 2018). However, basidiospore morphology (spherical to sub-elliptical) and Q values (1.0–1.23) of *H. luteoalbum*, *H. albotomentosum*, and *H. pallidomarginatum* differ significantly from the traditional diagnostic features of subgenus *Pallida* (ovoid to broadly elliptical basidiospores with Q > 1.25). Based on the latest phylogenetic data (Niskanen et al. 2018; Cao et al. 2021; Qin et al. 2024; Su et al. 2024; Zhang et al. 2024) incorporating newly generated sequencing data from this study, these three species are recovered in three strongly supported monophyletic clades within subgenus *Pallida*. This discrepancy between morphological traits and phylogenetic relationships indicates that the taxonomic diagnostic criteria for the subgenus may require re-evaluation. By integrating phylogenetic evidence with traditional morphological traits, such as basidioma morphology and spore parameters, we propose expanding the defined range of basidiospore Q values within subgenus *Pallida*.

Global *Hydnum* species exhibit significant regional distribution patterns: approximately 60% of known species, or 32 species, are concentrated in temperate regions such as Europe and North America, with only a few distributed in subtropical areas (Feng et al. 2016; Niskanen et al. 2018). Compared with the three early recorded species in China, recent studies have remarkably expanded the species diversity of this genus – currently, 32 *Hydnum* species have been reported in China, over half of which were newly discovered in subtropical regions such as Sichuan Province, Hunan Province, Hubei Province, and Anhui Province (Cao et al. 2021; Qin et al. 2024; Su et al. 2024; Zhang et al. 2024). This indicates that subtropical regions in China are also critical habitats for *Hydnum* species.

Additionally, as an ectomycorrhizal fungus, *Hydnum* forms stable symbiotic relationships with plants in the *Pinaceæ* (Agerer et al. 1996) and *Fagaceæ* (McNabb 1971; Feng et al. 2016; Niskanen et al. 2018) families, and its distribution is closely linked to that of its host plants (Niskanen et al. 2018; Swenie et al. 2018; Feng et al. 2016). Detailed recording of host species and other relevant information is of great significance for understanding the ecological distribution characteristics of species and habitat conservation (Durkin et al. 2020). The five species (*H. crassipedum*, *H. albomarginatum*, *H. fulvostriatum*, *H. bifurcatum*, and *H. orientalbidum*) we previously described (Tuo et al. 2025), together with the five species identified here, are all distributed in *Quercus* forests or *Quercus*-dominated forests. A comprehensive analysis of *Hydnum* species in China further indicates that nearly all species grow in *Pinus*–*Quercus* mixed forests or *Quercus*-dominated broad-leaved forests (Appendix 1). This suggests

a potential direct ecological association between *Hydnum* distribution and *Pinaceæ*/*Fagaceæ* – previous ectomycorrhizal tip sequencing studies have directly confirmed the ectomycorrhizal association between *Hydnum* and these plant families (Agerer et al. 1996; Tanaka and Nara 2009; Gao et al. 2013). From a regional distribution perspective, *Hydnum* species in China exhibit a pattern of "subtropical dominance with temperate supplementation": 20 species have been recorded in subtropical regions, while only four species are found in temperate regions. This distribution pattern is highly consistent with the geographical distributions of *Quercus* (Wang et al. 2022) and *Pinus* (Yue et al. 2025) in China. This indicates that subtropical and temperate regions – particularly the distribution ranges of *Quercus* and *Pinus* – may harbor rich *Hydnum* species resources, and strengthening the protection of habitats dominated by *Quercus* and *Pinus* should be an important practical direction for maintaining *Hydnum* species diversity.

Phenology is another key factor influencing fungal occurrence (Andrew et al. 2018; Krah et al. 2023). Although we conducted long-term macrofungal specimen sampling in the Dabie Mountains region from 2019 to 2024 (two to three times per week during April–October each year), *Hydnum* specimens were almost exclusively observed in August. Further analysis of the phenology of *Hydnum* species in China reveals that their peak occurrence mainly occurs from mid-August to mid-September (Appendix 1). This phenological characteristic is likely closely related to the precipitation and temperature conditions in this period of China – characterized by abundant rainfall and high temperatures (Zhan et al. 2019; Deng et al. 2022) – as suitable temperature and humidity conditions are conducive to spore germination (Setlow 2003) and mycelial growth (Querejeta et al. 2009). Ectomycorrhizal fungi act as symbiotic partners with plant roots, extracting water and inorganic nutrients from the soil through mycorrhizal hyphae and transferring them to the roots of the trees they colonize (Lehto and Zwiazek 2011). In return, the fungi receive carbohydrates from the host plants (Courty et al. 2010). The timing of carbohydrate uptake could potentially influence the phenology of the fruiting bodies (Sato et al. 2012). Consequently, ectomycorrhizal (EM) fungi are favored for fruiting body production during the host's active photosynthetic period, typically in the summer (Sato et al. 2012).

Acknowledgments

We sincerely extend our heartfelt gratitude to the Hefei Mycological Valley Innovation Institute, Forestry Bureau of Jinzhai County, Anhui Province, and the community of Tianma National Nature Reserve for their valuable support provided during the resource collection process. We sincerely thank the Subject Editor and reviewers for their valuable corrections and helpful suggestions on how to improve our work.

Additional information

Conflict of interest

The authors have declared that no competing interests exist.

Ethical statement

No ethical statement was reported.

Use of AI

No use of AI was reported.

Funding

This work was supported by the National Key Research and Development Program of China (No. 2024YFD1200204-4); the pilot selection projects in higher education institutions (No. 24GXYSZZ15); the 2024 Science and Technology Support Project of the Inner Mongolia Innovation Center of Biological Breeding Technology (2024NSZC01); Key R&D Program Project of Ordos City, Inner Mongolia Autonomous Region (YF20240036); Technology and demonstration of factory cultivation of Agaricus bisporus mushroom by high-value utilization of straw and livestock manure (No. 20230202121NC); the "111" Program (No. D17014); and the Hefei Mycological Valley Innovation Institute (jwg202307).

Author contributions

Yonglan Tuo: Conceptualization, Investigation, Data curation, Visualization, Writing – original draft. Hang Chu: Data curation and Software. Libo Wang: Investigation and Software. Jiajun Hu: Validation and Investigation. Zhengxiang Qi: Conceptualization and Methodology. Xiao Li: Funding acquisition, Project administration. Bo Zhang: Conceptualization, Project administration, Resources, and Writing – review and editing. Yu Li: Funding acquisition and Project administration.

Author ORCIDs

Yonglan Tuo https://orcid.org/0000-0001-6019-1038
Zhengxiang Qi https://orcid.org/0000-0002-0037-9407
Jiajun Hu https://orcid.org/0000-0002-7562-7612
Bo Zhang https://orcid.org/0000-0001-9508-8188
Yu Li https://orcid.org/0000-0003-4719-7210

Data availability

ML tree, BI tree, and alignment files have been uploaded to the online database figshare (https://doi.org/10.6084/m9.figshare.29858450; V2).

References

Agerer R, Kraigher H, Javornik B (1996) Identification of ectomycorrhizae of *Hydnum rufescens* on Norway spruce and the variability of the ITS region of *H. rufescens* and *H. repandum* (*Basidiomycetes*). Nova Hedwigia 63: 183–194. https://doi.org/10.1127/nova.hedwigia/63/1996/183

Andrew C, Heegaard E, Høiland K, Senn-Irlet B, Kuyper TW, Krisai-Greilhuber I, Kirk PM, Heilmann-Clausen J, Gange AC, Egli S, Bässler C, Büntgen U, Boddy L, Kauserud H (2018) Explaining European fungal fruiting phenology with climate variability. Ecology 99: 1306–1315. https://doi.org/10.1002/ecy.2237

Baird R, Wallace LE, Baker G, Scruggs M (2013) Stipitate hydnoid fungi of the temperate southeastern United States. Fungal Diversity 62: 41–114. https://doi.org/10.1007/s13225-013-0261-6

Banker HJ (1901) A preliminary contribution to a knowledge of the *Hydnaceæ*. Bulletin of the Torrey Botanical Club 28: 199–222. https://doi.org/10.2307/2478788

Banker HJ (1906) A contribution to a revision of the North American *Hydnaceæ*. Memoirs of the Torrey Botanical Club 12: 99–194. https://doi.org/10.5962/bhl.title.97394

Cao T, Hu YP, Yu JY, Wei TZ, Yuan HS (2021) A phylogenetic overview of the *Hydnaceæ* (*Cantharellales*, *Basidiomycota*) with new taxa from China. Studies in Mycology 99: 100121. https://doi.org/10.1016/j.simyco.2021.100121

Courty PE, Buée M, Diedhiou AG, Frey-Klett P, Le Tacon F, Rineau F, Turpault MP, Uroz S, Garbaye J (2010) The role of ectomycorrhizal communities in forest ecosystem processes: New perspectives and emerging concepts. Soil Biology & Biochemistry 42: 679–698. https://doi.org/10.1016/j.soilbio.2009.12.006

Deng HJ, Pepin N, Chen YN, Guo B, Zhang SH, Zhang YQ, Chen XW, Gao L, Liu MB, Chen Y (2022) Dynamics of diurnal precipitation differences and their spatial variations in China. Journal of Applied Meteorology and Climatology 61: 1015–1027. https://doi.org/10.1175/JAMC-D-21-0232.1

Durkin L, Jansson T, Sanchez M, Khomich M, Ryberg M, Kristiansson E, Nilsson RH (2020) When mycologists describe new species, not all relevant information is provided (clearly enough). MycoKeys 72: 109–128. https://doi.org/10.3897/mycokeys.72.56691

Feng B, Wang XH, Ratkowsky D, Gates G, Lee SS, Grebenc T, Yang ZL (2016) Multilocus phylogenetic analyses reveal unexpected abundant diversity and significant disjunct distribution pattern of the hedgehog mushrooms (*Hydnum* L.). Scientific Reports 6: 25586. https://doi.org/10.1038/srep25586

Gao C, Shi NN, Liu YX, Peay KG, Zheng Y, Ding Q, Mi XC, Ma KP, Wubet T, Buscot F, Guo LD (2013) Host plant genus level diversity is the best predictor of ectomycorrhizal fungal diversity in a Chinese subtropical forest. Molecular Ecology 22: 3403–3414. https://doi.org/10.1111/mec.12297

Gardes M, Bruns TD (1993) ITS primers with enhanced specificity for basidiomycetes application to the identification of mycorrhizae and rusts. Molecular Ecology 2: 113–118. https://doi.org/10.1111/j.1365-294X.1993.tb00005.x

Grebenc T, Martín MP, Kraigher H (2009) Ribosomal ITS diversity among the European species of the genus "*Hydnum*" (*Hydnaceæ*). Anales del Jardín Botánico de Madrid. Real Jardín Botánico, 121–132. https://doi.org/10.3989/ajbm.2221

Guindon S, Dufayard JF, Lefort V, Anisimova M, Hordijk W, Gascuel O (2010) New algorithms and methods to estimate maximum-likelihood phylogenies: Assessing the performance of PhyML 3.0. Systematic Biology 59: 307–321. https://doi.org/10.1093/sysbio/syq010

Hall TA (1999) BioEdit: S user-friendly biological sequence alignment editor and analysis program for windows 95/98/nt. Nucleic Acids Symposium Series 41: 95–98. https://doi.org/10.1021/bk-1999-0734.ch008

Hall D, Stuntz D (1971) Pileate hydnaceae of the puget sound area. I. White-spored genera: *Auriscalpium*, *Hericium*, *Dentinum* and *Phellodon*. Mycologia 63: 1099–1128. https://doi.org/10.1080/00275514.1971.12019214

Huhtinen S, Ruotsalainen J (2006) Variability of *Hydnum rufescens* in Finland: Three taxa hidden under one name–and appearance. Karstenia 46: 17–24. https://doi.org/10.29203/ka.2006.412

Justo A, Hood AW, Swenie RA, Matheny PB (2023) *Hydnum atlanticum*, a new species from Eastern North America. Fungal Systematics and Evolution 11: 63–70. https://doi.org/10.3114/fuse.2023.11.05

Kalyaanamoorthy S, Minh BQ, Wong TKF, von Haeseler A, Jermiin LS (2017) ModelFinder: Fast model selection for accurate phylogenetic estimates. Nature Methods 14: 587–589. https://doi.org/10.1038/nmeth.4285

Katoh K, Standley DM (2013) MAFFT multiple sequence alignment software version 7: Improvements in performance and usability. Molecular Biology and Evolution 30: 772–780. https://doi.org/10.1093/molbev/mst010

Kim JS, Lee W, Kim C, Park H, Kim CS, Lim YW (2023) Unveiling the diversity of *Hydnum* in the Republic of Korea with one new species, *Hydnum paucispinum*. Mycobiology 51: 300–312. https://doi.org/10.1080/12298093.2023.2265137

Kornerup A, Wanscher JHK (1978) The Methuen Handbook of Colour (3rd edn.). Methuen Publishing Ltd, London, 256 pp.

Krah FS, Büntgen U, Bässler C (2023) Temperature affects the timing and duration of fungal fruiting patterns across major terrestrial biomes. Ecology Letters 26: 1572–1583. https://doi.org/10.1111/ele.14275

Leebens-Mack J, Vision T, Brenner E, Bowers JE, Cannon S, Clement MJ, Cunningham CW, dePamphilis C, deSalle R, Doyle JJ, Eisen JA, Gu X, Harshman J, Jansen RK, Kellogg EA, Koonin EV, Mishler BD, Philippe H, Pires JC, Qiu YL, Rhee SY, Sjölander K, Soltis DE, Soltis PS, Stevenson DW, Wall K, Warnow T, Zmasek C (2006) Taking the first steps towards a standard for reporting on phylogenies: Minimum Information About a Phylogenetic Analysis (MIAPA). Omics : A Journal of Integrative Biology 10: 231–237. https://doi.org/10.1089/omi.2006.10.231

Lehto T, Zwiazek JJ (2011) Ectomycorrhizas and water relations of trees: A review. Mycorrhiza 21: 71–90. https://doi.org/10.1007/s00572-010-0348-9

Márquez-Sanz R, Gorjón SP, Salcedo I, Olariaga I (2023) *Hydnum pallidum* Raddi, the correct name for *H. albidum* Peck in the sense of European authors and the recently described *H. reginæ* Kibby, Liimat. & Niskanen. Journal of Fungi 9: e1141. https://doi.org/10.3390/jof9121141

Massee G (1910) Fungi exotici: XI. Bulletin of Miscellaneous Information (Royal Botanic Gardens, Kew) 1910: 249–253. https://doi.org/10.2307/4111851

McNabb RFR (1971) Some new and revised taxa of New Zealand Basidiomycetes (Fungi). New Zealand Journal of Botany 9: 355–370. https://doi.org/10.1080/002882 5X.1971.10429148

Moeller HV, Peay KG, Fukami T (2014) Ectomycorrhizal fungal traits reflect environmental conditions along a coastal California edaphic gradient. FEMS Microbiology Ecology 87: 797–806. https://doi.org/10.1111/1574-6941.12265

Moncalvo JM, Nilsson RH, Koster B, Dunham SM, Bernauer T, Matheny PB, Porter TM, Margaritescu S, Weiß M, Garnica S (2006) The cantharelloid clade: Dealing with incongruent gene trees and phylogenetic reconstruction methods. Mycologia 98: 937–948. https://doi.org/10.1080/15572536.2006.11832623

Nguyen LT, Schmidt HA, von Haeseler A, Minh BQ (2015) IQ-TREE: A fast and effective stochastic algorithm for estimating maximum-likelihood phylogenies. Molecular Biology and Evolution 32: 268–274. https://doi.org/10.1093/molbev/msu300

Nilsson RH, Larsson KH, Larsson E, Kõljalg U (2006) Fruiting body-guided molecular identification of root-tip mantle mycelia provides strong indications of ectomycorrhizal associations in two species of *Sistotrema* (*Basidiomycota*). Mycological Research 110: 1426–1432. https://doi.org/10.1016/j.mycres.2006.09.017

Niskanen T, Liimatainen K, Nuytinck J, Kirk P, Ibarguren IO, Garibay-Orijel R, Norvell L, Huhtinen S, Kytövuori I, Ruotsalainen J (2018) Identifying and naming the currently known diversity of the genus *Hydnum*, with an emphasis on European and North

American taxa. Mycologia 110: 890–918. https://doi.org/10.1080/00275514.2018.1477004

Olariaga I, Grebenc T, Salcedo I, Martín MP (2012) Two new species of *Hydnum* with ovoid basidiospores: *H. ovoideisporum* and *H. vesterholtii*. Mycologia 104: 1443–1455. https://doi.org/10.3852/11-378

Ostrow H, Beenken L (2004) *Hydnum ellipsosporum* spec. nov. (*Basidiomycetes*, *Cantharellales*)–ein doppelgänger von *Hydnum rufescens* Fr. Zeitschrift für Mykologie 70: 137–156.

Qin HZ, Liao YT, Zhang YZ, Lin WF, Yang XQ, Zeng NK (2024) A contribution to the knowledge of *Hydnum* (*Hydnaceæ*, *Cantharellales*) in China, introducing a new taxon and amending descriptions of five known species. Diversity 16: e166. https://doi.org/10.3390/d16030166

Querejeta J, Egerton-Warburton LM, Allen MF (2009) Topographic position modulates the mycorrhizal response of oak trees to interannual rainfall variability. Ecology 90: 649–662. https://doi.org/10.1890/07-1696.1

Ronquist F, Teslenko M, van der Mark P, Ayres DL, Darling A, Höhna S, Larget B, Liu L, Suchard MA, Huelsenbeck JP (2012) MrBayes 3.2: Efficient bayesian phylogenetic inference and model choice across a large model space. Systematic Biology 61: 539–542. https://doi.org/10.1093/sysbio/sys029

Sato H, Morimoto S, Hattori T (2012) A thirty-year survey reveals that ecosystem function of fungi predicts phenology of mushroom fruiting. PLoS ONE 7: e49777. https://doi.org/10.1371/journal.pone.0049777

Setlow P (2003) Spore germination. Current Opinion in Microbiology 6: 550–556. https://doi.org/10.1016/j.mib.2003.10.001

Su LJ, Yu TJ, Xue R, Zhang WH, Xu C, Xia X, Li J, Lei HC, Yang D, Zhang GL, Tang LP (2024) New contributions on species diversity of genus *Hydnum* and *Lentaria* sl in China. Journal of Fungi 10: e824. https://doi.org/10.3390/jof10120824

Sugawara R, Maekawa N, Sotome K, Nakagiri A, Endo N (2022) Systematic revision of *Hydnum* species in Japan. Mycologia 114: 413–452. https://doi.org/10.1080/00275514.2021.2024407

Swenie RA, Baroni TJ, Matheny PB (2018) Six new species and reports of *Hydnum* (*Cantharellales*) from eastern North America. MycoKeys 42: 35–72. https://doi.org/10.3897/mycokeys.42.27369

Tanaka M, Nara K (2009) Phylogenetic diversity of non-nodulating Rhizobium associated with pine ectomycorrhizae. FEMS Microbiology Ecology 69: 329–343. https://doi.org/10.1111/j.1574-6941.2009.00720.x

Tuo YL, Wang LB, Li XF, Chu H, Liu MH, Hu JJ, Qi ZX, Li X, Li Y, Zhang B (2025) New contributions to the species diversity of the genus *Hydnum* (*Hydnaceæ*, *Cantharellales*) in China: Four new taxa and newly recorded species. Journal of Fungi 11: e431. https://doi.org/10.3390/jof11060431

Vizzini A, Picillo B, Ercole E, Voyron S, Contu M (2013) Detecting the variability of *Hydnum ovoideisporum* (*Agaricomycetes*, *Cantharellales*) on the basis of Italian collections, and *H. magnorufescens* sp. nov. Mycosphere: Journal of Fungal Biology 4: 32–44. https://doi.org/10.5943/mycosphere/4/1/2

Wang XH, Das K, Horman J, Antonin V, Baghela A, Chakraborty D, Hembrom ME, Nakasone K, Ortiz-Santana B, Vizzini A (2018) Fungal biodiversity profiles 51–60. Cryptogamie. Mycologie 39: 211–257. https://doi.org/10.7872/crym/v39.iss2.2018.211

Wang Y, Xu CY, Wang Q, Jiang YR, Li Q (2022) Germplasm resources of oaks (*Quercus* L.) in China: Utilization and prospects. Biology 12: 1–76. https://doi.org/10.3390/biology12010076

White TJ, Bruns T, Lee S, Taylor J (1990) Amplification and direct sequencing of fungal ribosomal RNA genes for phylogenetics. PCR Protocols: a Guide to Methods and Applications 18: 315–322. https://doi.org/10.1016/B978-0-12-372180-8.50042-1

Xiang CY, Gao FL, Jakovlić I, Lei HP, Hu Y, Zhang H, Zou H, Wang GT, Zhang D (2023) Using PhyloSuite for molecular phylogeny and tree based analyses. iMeta 2: e87. https://doi.org/10.1002/imt2.87

Xie Y, MacKinnon J, Li DM (2004) Study on biogeographical divisions of China. Biodiversity and Conservation 13: 1391–1417. https://doi.org/10.1023/B:BIOC.0000019396.31168.ba

Xu BC, Pan JH (2019) Spatial distribution characteristics of national protected areas in China. Journal of Geographical Sciences 29: 2047–2068. https://doi.org/10.1007/s11442-019-1704-0

Yanaga K, Sotome K, Ushijima S, Maekawa N (2015) *Hydnum* species producing whitish basidiomata in Japan. Mycoscience 56: 434–442. https://doi.org/10.1016/j.myc.2015.01.001

Ying JZ, Zang M (1994) Economic Macrofungi from Southwestern China. Science Press, Beijing, China, 53 pp.

Yue JJ, Zhang HY, Zhao L, Wang ZY, Zou HC, Liu Z (2025) Historical climate change drives species richness patterns of *Pinus* L. in China. Biodiversity and Conservation 34: 2177–2195. https://doi.org/10.1007/s10531-025-03069-y

Zang M, Li B, Xi J, Zhang D (1996) Fungi of Hengduan Mountains. Science Press, Beijing, China, 105 pp.

Zhan MJ, Xia LJ, Zhan LF, Wang YH (2019) Recognition of changes in air and soil temperatures at a station typical of China's subtropical monsoon region (1961–2018). Advances in Meteorology: e6927045. https://doi.org/10.1155/2019/6927045

Zhang M, Wang CQ, Bai HF, Deng WQ (2024) A contribution to the phylogeny and taxonomy of *Hydnum* (*Cantharellales*, *Basidiomycota*) from China. Journal of Fungi 10: 1–98. https://doi.org/10.3390/jof10020098

Appendix 1

Table A1. Morphological comparison of *Hydnum* species in China.

Species	Pileus		Spines		Spores			Habitat	Time	Distribution	References
	Color	Size (cm)	Color	Length (mm)	Size (μm)	av. L × W (μm)	Q				
H. albodentum	brownish orange to light brown	27.5–55.5	white	3–10	(7.0) 8–8.5 (9) × (5.5) 6.0–7.0 (8.0)	avg. 7.93 × 6.78	Q = 1.13–1.25	*Q. serrata* and *C. lanceolata* mix forests	September	Anhui China	This study
H. albomagnum	Cream-white to pale cream	25–60	Cream-white to pale cream	6–12	(4.6) 4.8–6.7 (7.1) × (3.5) 3.9–5.4 (5.6)	avg. 5.0–6.5 × 4–5.5	Q = 1.07–1.36	Hardwood-oak forests	September	Hunan China, Japan	(Cao et al. 2021)
H. albomarginatum	Yellowish-white	23–66	Pale cream	2–6	(7.0) 8.0–8.5 (9.0) × (7.0) 8.0–8.2 (9.0)	avg. 8.04 × 7.93	Q = 1.00–1.09	*Quercus serrata* forests	October	Anhui China	(Tuo et al. 2025)
H. albotomentosum	white to pale yellow	22–30	white to yellowish white	0.5–2	(6)7–8(8.5) × (5.5)6.5–7(8)	avg. 7.11 × 6.72	Q = 1.0–1.14	*Q. variabilis* and *P. hwangshanensis* forests	August	Anhui China	This study
H. berkeleyanum	Pale orange to light orange	25–80	Orange-white	2–9	(7.5) 8.4–8.5 (9.5) × (6.9) 7.9–8 (8.8)	avg. 8.4 × 7.95	Q = 1.01–1.17	*Q. serrata* forest	August	India, Yunnan, Anhui China	This study
H. bifurcatum	Pale cream	65–135	Yellowish-white	2–7	(8.0) 8.5–9.5 (10.0) × (7.5) 8.0–9.5 (10.0)	avg. 9.12 × 8.97	Q = 1.00–1.06	*Q. mongolica* forests	September	Jilin China	(Tuo et al. 2025)
H. brevispinum	Yellowish-white	10–15	Pure white	0.2–0.8	(4.5) 5.0–5.8 (6.0) × (3.5) 3.8–4.8 (5.0)	avg. 5.28 × 4.16	Q = 1.27–1.31	Angiosperm forests	September	Hunan Province	(Cao et al. 2021)
H. crassipedum	Yellowish-white to orange-white	24–56	Yellowish	2–5	(7.0) 8.0–8.5 (9.0) × (6.5) 7.0–7.5 (6.0)	avg. 8.0 × 6.99	Q = 1.11–1.17	*Q. variabilis* forests	September	Anhui China	(Tuo et al. 2025)
H. cremeoalbum	White to cream-white	60–90	Yellowish-white	2–5	4.5–5.5 × 3.0–4.5	avg. 4.73 × 3.88	Q = 1.1–1.43	Broad-leaved and Mixed forests	August	Hubei, hainan, Hunan, Chongqing, Guangdong, China, Japan	(Qin et al. 2024)
H. cremeum	Warm cream to yellowish-white	25–37	Cream-yellow	4–5	8.1–9.5 × 7.1–9.0 (9.5)	avg. 8.8 × 8.05	Q = 1.00–1.11	Mixed forests	October	Yunnan China	(Su et al. 2024)
H. erectum	Creamy yellow to pale salmon	35–45	White to pale salmon	1–2	(6.5) 7.33–8.0 × (5.5) 6.68–7.5 (8.0)	avg. 7.67 × 7.09	Q = 1.0–1.125	*Fagaceæ* forests	August	Zhejiang China	(Qin et al. 2024)
H. flabellatum	Yellow to grayish-yellow	30–45	Orange-white	0.6–2	(7.8) 8.5–9.5 (10.0) × (6.0) 6.5–7.8 (8.0)	avg. 9.07 × 7.04	Q = 1.26–1.29	Mixed forests	September	Liaoning China	(Cao et al. 2021)
H. flavidocanum	Yellowish-white or yellowish-gray	20–30	Orange-white	0.5–2	(7.0) 7.2–8.8 (8.9) × (5.2) 5.5–6.5 (6.8)	avg. 7.75 × 6.01	Q = 1.29–1.31	Mixed forests	August	Yunnan China	(Cao et al. 2021)
H. flavoquamosum	Light yellow to light brownish-orange	50	Light yellow to light brownish-orange	0.5	8.6–9.5 (10.0) × 7.6–8.6 (9.0)	avg. 9.05 × 8.1	Q = 1.05–1.23	Mixed forests	August	Yunnan China	(Su et al. 2024)
H. fulvostriatum	Yellowish-white	44–65	White	2–7	(6.8) 7–7.2 (8) × (6.5) 6.8–7.0 (7.5)	avg. 7.2 × 6.9	Q = 1.00–1.08	*Q. glauca* forests	August	Anhui China	(Tuo et al. 2025)
H. jussii	Medium orange ocher	60	Whitish		7.2–8.0 × 6.6–7.5	avg. 7.5 × 7.0	Q = 1.03–1.18	Coniferous forests		Finland, Sichuan, Xinjinag China	(Cao et al. 2021)
H. longibasidium	Orange-white to grayish orange	10–15	Orange-white to pale orange	1–4	(8.0) 8.5–11.0 (11.5) × (7.5) 7.8–9.8 (10.0)	avg. 9.81 × 9.03	Q = 1.09–1.13	Angiosperm forests	September	Hunan China	(Cao et al. 2021)

Species	Pileus		Spines		Spores			Habitat	Time	Distribution	References
	Color	Size (cm)	Color	Length (mm)	Size (μm)	av. L × W (μm)	Q				
H. longipes	Orange, light orange	20–30	Orange-white to pale orange	1–3	(7.5) 8.0–10.0 (10.5) × (6.0) 7.0–8.5 (9.0)	avg. 9.32 × 7.63	Q = 1.05–1.43	*Q. aquifolioides* and *Pinus densata* forests	September	Yunnan China	(Zhang et al. 2024)
H. luteoalbum	pale yellow to deep orange	25–30	white to yellowish white	5–10	(6.0)7.0–7.5(8.0) × (5.5)6.0–6.5(7.0)	avg. 7.08 × 6.10	Q = 1.08–1.17	*Q. serrata* forest	August	Anhui China	This study
H.melitosarx	Light orange to orange	20–40	Yellowish-white to pale orange	2–5	8.0–11.0 × 7.0–10.0	avg. 9.37 × 8.71	Q = 1.0–1.28	Broad-leaved and Mixed forests	August September	Europe, Sichuan China	(Zhang et al. 2024)
H. microcarpum	Yellowish-white to orange-white	10–20	White to yellowish-white	0.5–1.5	5.0–6.0 (6.5) × 5.0–5.5 (6.0)	avg. 5.78 × 5.26	Q = 1.0–1.2	Mixed forests	May	Guangdong China	(Zhang et al. 2024)
H. minum	Cream-yellow to pale buff	10–25	Cream yellow	0.5–1.7	4.5–5.5 × 3.0–4.5	avg. 4.8 × 3.8	Q = 1.1–1.5	Angiosperm forests	September	Hunan China, Japan	(Cao et al. 2021)
H. minus	Cream-white to cream	30–45	White to cream-white	2–4	(4.0) 4.72–5.0 × (3) 3.68–4.0	avg. 4.0–5.0 × 3.0–4.0	Q = 1.13–1.29	*Fagaceæ* forest	July August	Hainan, Yunan Hunan China, Japan	(Qin et al. 2024)
H. orientalbidum	White	30–45	White	1–3	(4.0) 4.5–5 (6.0) × (4.0) 4.5–5.0 (6.0)	avg. 4.6 × 4.4	Q = 1.0–1.11	Broad-leaved and *Q. serrata* forests	June October	Japan, Sichuan, Anhui, zhejian China	(Tuo et al. 2025)
H. pallidocroceum	Orange-white to pale orange	25–40	Light yellow	1–5	(7.5) 7.8–9.5 (10.0) × (5.5) 6.0–7.5 (8.0)	avg. 9.09 × 6.72	Q = 1.32–1.35	*Pinus* sp. forests	August	Xinjiang China	(Cao et al. 2021)
H. pallidomarginatum	Orange-white to pale orange	20–35	Orange-white to pale orange	0.5–2	(8.0) 8.2–9.8 (10.0) × (6.0) 6.5–7.8 (8.2)	avg. 8.75 × 6.99	Q = 1.25–1.28	*Q. serrata* forest	August	Yunnan, Anhui China	This study
H. pinicola	Pale yellow to pale orange	25–60	Orange-white to pale orange	1.5–3	4.0–6.0 × 3.5–5.0	avg. 4.72 × 4.02	Q = 1.0–1.25	Mixed forests	September October	Japan, Hubei, Yunnan China	(Zhang et al. 2024)
H. roseoalbum	Cream to whitish	65	Pale orange		8.1–9.0 (9.5) × 8.1–9.0		Q = 1.00–1.06	Broad-leaved forests	October	Yunnan China	(Su et al. 2024)
H. roseotangerinum	Pale brownish-orange	65	Yellowish-orange to pinkish-orange	4–5	8.6–9.5 (10.0) × 7.6–9.0	avg. 9.05 × 8.3	Q = 1.00–1.18	Mixed forests	August	Yunnan China	(Su et al. 2024)
H. sinorepandum	Light yellow to light orange	40–120	White to yellowish-white	3–7	(7.5) 8–9 (10) × 6.5–7.5	avg. 8.16 × 7.12	Q = 1.0–1.38	Broad-leaved and Mixed forests	September	Yunnan China	(Zhang et al. 2024)
H. sphæricum	Orange-white	20–35	White	0.5–3	(7.5) 8–8.8 (9) × (6) 6.5–7.5 (8)	avg. 8.36 × 6.94	Q = 1.2–1.23	Angiosperm forests	September	Hunan China	(Cao et al. 2021)
H. tangerinum	Orange to brownish-orange	10–50	Orange-white	2–6	(7) 7.2–8.8 (9) × (5.5) 5.8–7 (7.5)	avg. 8.11 × 6.19	Q = 1.23–1.31	Angiosperm forests	September	Hunan China	(Cao et al. 2021)
H. tenuistipitum	Yellow white to orange-white	10–30	Orange-white	1–3	(6.5) 6.8–7.2 (7.5) × (5.2) 5.5–6.5 (6.8)	avg. 7.08 × 6.09	Q = 1.07–1.16	Angiosperm forests	September	Hunan China	(Cao et al. 2021)
H. treui	White to creamy white	28–57	White to cream-white	1–4	(6) 6.44–7 (7.5) × (5) 5.88–6.5 (7)		Q = 1.0–1.2	*Fagaceæ* forests	September	Hainan China, Papua, New Guinea	(Qin et al. 2024)
H. ventricosum	Orange to brown	28–35	Orange-white	1–5	(7.5) 8.2–9 (9.5) × (7) 7.5–8.5 (9)	avg. 8.64 × 8.17	Q = 1.05–1.09	Mixed forests	August	Liaoning China	(Cao et al. 2021)
H. vesterholtii	Ocher to light ocher	10–50	Pale ocher	1–1.7	(7) 8–9 (9.5) × 6–7.5 (8)	avg. 8.2–8.7 × 6.4–6.8	Q = 1.27–1.3	*Abies alba* and *Fagus sylvatica* forests		Sichuan China, France	(Zhang et al. 2024)

Appendix 2

Characteristics of basidia and basidiospores as seen under a light microscope.

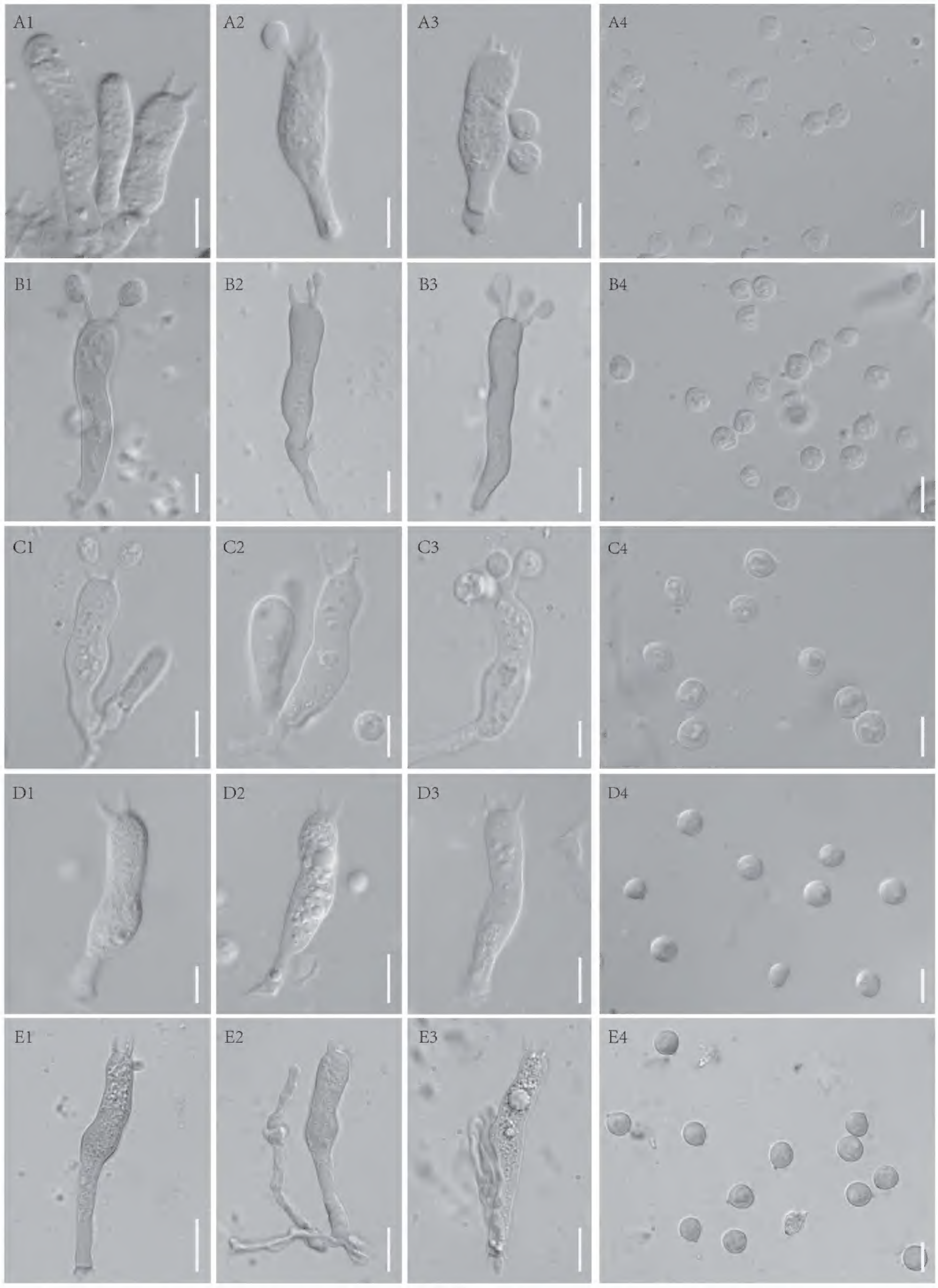

Figure A1. Microscopic features of basidia and basidiospores (**A1–E4**). **A1–A4.** *H. luteoalbum*; **B1–B4.** *H. albotomentosum*; **C1–C4.** *H. albodentum*; **D1–D4.** *H. pallidomarginatum*; **E1–E4.** *H. berkeleyanum*. Scale bars: 10 μm (**A1–E4**).